ALKALOID EXTRACT OF *AGERATINA ADENOPHORA* STEM AS GREEN CORROSION INHIBITOR FOR MILD STEEL CORROSION IN 1M H_2SO_4 ACID SOLUTION

A DISSERTATION SUBMITTED FOR THE PARTIAL FULFILLMENT OF THE REQUIREMENTS FOR THE MASTER OF SCIENCE DEGREE IN CHEMISTRY

SUBMITTED BY

Name: JAMUNA THAPA MAGAR

T.U. Examination Roll No.: 1881/076

T.U. Registration No: 5-2-33-238-2014

SUBMITTED TO

DEPARTMENT OF CHEMISTRY

AMRIT CAMPUS

INSTITUTE OF SCIENCE AND TECHNOLOGY

KATHMANDU, NEPAL

June 2023

BOARD OF EXAMINER AND CERTIFICATE OF APPROVAL

This dissertation entitled, **"Alkaloid Extract of *Ageratina adenophora* Stem as Green Corrosion Inhibitor for Mild Steel Corrosion in 1M H_2SO_4 Solution"** by **Ms. Jamuna Thapa Magar** under the supervision of Asst. Prof. Hari Bhakta Oli, Department of Chemistry, Amrit Campus, Tribhuvan University, Kathmandu, Nepal, and under co-supervision of Asst. Prof. Dr. Deval Prasad Bhattarai, Department of Chemistry, Amrit Campus, Tribhuvan University, Kathmandu, Nepal, hereby submitted has been approved for partial fulfillment of the requirement for completion of her Master of Science (M.Sc.) Degree in Chemistry. This dissertation has not been submitted to any other university or institution previously for the award of a degree.

.....

Supervisor
Asst. Prof. Hari Bhakta Oli
Department of Chemistry
Amrit Campus, TU, Kathmandu, Nepal

.....

Co-supervisor
Asst. Prof. Dr. Deval Prasad Bhattarai
Department of Chemistry
Amrit Campus, TU, Kathmandu, Nepal

.....

External Examiner
Prof. Dr. Amar Prasad Yadav
Central Department of Chemistry
TU, Kathmandu, Nepal

.....

Internal Examiner
Assoc. Prof. Dr. Ram Lal Shrestha
Department of Chemistry
Amrit Campus, TU, Kathmandu, Nepal

Tribhuvan University
Amrit Campus
Department of Chemistry

.....

Head of the Department
Assoc. Prof. Kanchan Sharma
Department of Chemistry
Amrit Campus, TU, Kathmandu, Nepal

.....

M.Sc. Chemistry Coordinator
Assoc. Prof. Dr. Bhushan Shakya
Department of Chemistry
Amrit Campus, TU, Kathmandu, Nepal

Date: July 5, 2023

LETTER OF RECOMMENDATION

This is to recommend that the dissertation work entitled "**Alkaloid Extract of *Ageratina adenophora* Stem as Green Corrosion Inhibitor for Mild Steel Corrosion in 1M H_2SO_4 solution**" has been carried out by **Ms. Jamuna Thapa Magar** as partial fulfillment for the requirement of Master of Science Degree in Chemistry. This is her original work and has been carried out under our guidance and supervision. To the best of our knowledge, this research has not been submitted for any other degree at any other institute.

Supervisor

Asst. Prof. Hari Bhakta Oli

Department of Chemistry

Amrit Campus, T.U.

Kathmandu, Nepal

Co-Supervisor

Asst. Prof. Dr. Deval Prasad Bhattarai

Department of Chemistry

Amrit Campus, T.U.

Kathmandu, Nepal

Tribhuvan University
Amrit Campus
Department of Chemistry

Date: June 25, 2023

DECLARATION

I, Jamuna Thapa Magar, hereby declare that the work entitled "**Alkaloid Extract of *Ageratina adenophora* Stem as Green Corrosion Inhibitor for Mild Steel Corrosion in 1M H_2SO_4 solution**" submitted to the Institute of Science and Technology Tribhuvan University as partial fulfillment for the requirements of Master of Science Degree in Chemistry has been originally done by me and has not been submitted earlier in part or full in this or any other form to any other university/institute, here or elsewhere for the award of any degree. All sources of information have been specifically acknowledged by reference to the authors or institutions.

Jamuna Thapa Magar
Symbol No: 1881/076
TU Registration No: 5-2-33-238-2014

June 25, 2023

ACKNOWLEDGEMENTS

I would like to express my profound gratitude, deep honor, and appreciation to my respected supervisor, Asst. Prof. Hari Bhakta Oli, and Co-supervisor, Asst. Prof. Dr. Deval Prasad Bhattarai for their guidance, invaluable suggestions, kind support, and regular encouragement during the entire period of this dissertation's research and writing. My appreciation goes to Assoc. Prof. Kanchan Sharma, Head of the Department of Chemistry, Amrit Campus, and Assoc. Prof. Dr. Bhushan Shakya**,** co-ordinator of the M.Sc. program, Amrit Campus, for their generous support to complete this work in time.

I would like to express my gratitude to the Central Department of Chemistry, Tribhuvan University for their assistance in the electrochemical measurements, and special thanks to Prof. Dr. Amar Prasad Yadav and Asst. Prof. Anju Kumari Das for helping me with polarization and electrochemical impedance measurements to complete a major proportion of this dissertation.

I thank my teachers, administrative staff, colleagues, and others for their kind help and cooperation during my research period. I am obliged to my family members who have been a great source of inspiration to me. Also, I would like to convey my deep appreciation to Simone and Roman Gilg for their utmost love and support.

Jamuna Thapa Magar
June 25, 2023

ABSTRACT

Green corrosion inhibitors are environmentally friendly, biodegradable, and renewable compounds that are used to prevent corrosion in metals and alloys. In this study, the alkaloid from the stem of *Ageratina adenophora* (AA) was successfully extracted through the cold percolation and solvent extraction methods, chemically and spectroscopically characterized, and investigated as an inhibitor for mild steel (MS) corrosion in 1M H_2SO_4 solution. The thermodynamics, kinetics, and corrosion mechanism were studied from the weight loss measurements and electrochemical techniques such as potentiodynamic polarization (PDP) and electrochemical impedance spectroscopy (EIS). The EIS experiment showed increments in the charge transfer resistance as the concentration of inhibitor increased and reaches the maximum inhibition efficiency of 93% for the 800 ppm inhibitor solution at 293 K. Adsorption of inhibitor compounds on the MS interface appeared as the major physisorption, according to the adsorption isotherm analysis. Moreover, the adsorption of the inhibitor molecules strongly obeys the Langmuir isotherm model.

Keywords: *Ageratina adenophora,* alkaloids, corrosion inhibitor, weight loss, adsorption isotherm, polarization.

LIST OF ABBREVIATIONS

ΔG_{ads}	Gibbs Free Energy of Adsorption
AA	*Ageratina adenophora*
C_{inh}	Concentration of Inhibitors
CPE	Constant Phase Element
CR	Corrosion Rate
E_a	Activation Energy
EIS	Electrochemical Impedance Spectroscopy
FTIR	Fourier Transform Infrared Spectroscopy
IE	Inhibition Efficiency
K_{ads}	Langmuir adsorption equilibrium
kJ/mol	Kilojoule per mole
MS	Mild Steel
mV/s	Millivolt per second
OCP	Open Circuit Potential
PDP	Potentiodynamic Potential
R_{ct}	Charge Transfer Resistance
$R_{ct(inh)}$	Charge Transfer Resistance of Inhibitor molecules
R_s	Solution Resistance
UV	Ultra Violet
Θ	Fraction of Surface Coverage
SCE	Saturated Calomel Electrode
ppm	Parts per million

LIST OF TABLES

LIST OF FIGURES

TABLE OF CONTENTS

CHAPTER 1

INTRODUCTION

1.1 Corrosion

The literal meaning of corrosion has a Latin origin from "*corrodere"* often referring to "gnawing to pieces", "to chew away", or "to attack" (Landolt, 2007; Sastri, 2011). International Organization for Standardization (ISO) 8044: 2020 defines corrosion as a metallic material's physical-chemical interaction with its surroundings that alters the metal's characteristics and could potentially harm the function of the metal, the environment, or the technological system that these components are a part of (https://www.iso.org). Corrosion is also described by the International Union of Pure and Applied Chemistry (IUPAC, 1997) as an irreversible interfacial physicochemical interaction of the material with the surrounding environment causing material consumption or the dissolution of an environmental component into the substance. This general approach compiles both the positive and negative aspects of corrosion while excluding some physical or mechanical processes (Landolt, 2007). There are various forms of corrosion based on the corrosion phenomena (Fontana, 1986). Some examples of phenomenological corrosion attacks involve rusting of iron, silver tarnishing, cracking in brass by ammonia, dissolution of mineral glass by alkaline, etc. (Landolt, 2007).

An electrochemical mechanism is the fundamentals of corrosion involving chemical species and electrons in the oxidation (anodic) and reduction (cathodic) reactions. A generic corrosion reaction of a metal, M is (Pedeferri & Ormellese, 2018),

$$\mathrm{M} + \text{aggressive environment} \rightarrow \text{corrosion products} \tag{1.1}$$

A generic anodic corrosion reaction involves the transfer of metal cations into the solution. As a result, electrons are released onto the metal surface (Groysman, 2010).

$$\mathrm{M_{(s)}} = \mathrm{M^{z+}_{(aq)}} + \mathrm{ne^-} \tag{1.2}$$

Where $\mathrm{M^{z+}_{(aq)}}$ is the metallic cations.

A generic cathodic corrosion reaction involves the gain of electrons by the chemical species, D (Groysman, 2010).

$$\mathrm{D_{(aq)}} + \mathrm{ne^-} \rightarrow \mathrm{D^{n-}_{(aq)}} \tag{1.3}$$

Where $D^{n-}_{(aq)}$ is the metallic anion.

Some cathodic corrosion reactions are (Pedeferri & Ormellese, 2018):

a) Hydrogen evolution reaction: $H^+ + e^- = H$ or $2H^+ + 2e^- = H_2$ (1.4)

b) Oxygen reduction reaction: $O_2 + 2H_2O + 4e^- = 4OH^-$ (1.5)

$$O_2 + 4H^+ + 4e^- = 2H_2O \quad (1.6)$$

Both the anodic and cathodic processes involve simultaneously one after another.

1.2 Significance of Corrosion

Corrosion is accepted as an inescapable universal adversary due to its detrimental and threatening nature, particularly for metallic materials. Which plays a vital role in the modern, mechanized, industrial, and technologically advanced period (Roberge, 2008). The major corrosion failures involve compromised safety, efficiency, energy, productivity losses, and environmental concerns (Revie and Uhlig, 2008). The strategic impact of corrosion can be described as follows:

a) Energy impact: Internationally, the energy needed to produce one ton of steel is roughly equivalent to the amount used by a typical family over the course of three months while one ton of steel rusts away within a moment (Javaherdashti, 2000).

b) Economic impact: The economic impact of corrosion in different countries is different. For instance, the economic loss due to metallic corrosion is US$900 million in Saudi Arabia, US$310 billion in China, and US$26.1 billion in India respectively (Hou *et al*., 2017; Koch, 2017). While in Nepal, the total annual cost of corrosion amounts to almost 4.3% of the GDP (Karki, 2021).

   i) Direct impact: The cost of inspection, maintenance, replacement, and repair of corroded structures and machinery often exceeds the price of the material itself (Landolt, 2007).

   ii) Indirect impact: This includes shutdown, public service interruptions, loss of both product and efficiency, accidents, overdesign, toxic chemicals release, product contamination, and other issues (Petrovic, 2016; Revie and Uhlig, 2008).

c) Environmental impact/health: Several catastrophic events cause environmental pollution, death, and material loss (Javaherdashti, 2000).

However, corrosion can be favorable and desirable in some processes (Landolt, 2007). These are listed as follows:

- Plays a vital role in eliminating abandoned metallic materials naturally.
- For industrial manufacturing, corrosion reactions are important.
- Creation of a smooth metallic surface through the chemical and electrochemical polishing corrosion reactions.
- For the anodization of aluminum to obtain natural oxide film formation to improve corrosion resistance.

1.3 Mild steel (MS) corrosion and sulfuric acid

Mild steel (MS) is a type of ferrous metal containing 0.05-0.25% carbon that is more favored, frequently utilized, and cheaply priced metallic material for various structural applications due to its mechanical, magnetic, thermal, and electrochemical qualities (Thapa *et al.*, 2022). Mostly the structural and compositional units of metal are the basics for predicting its corrosion behavior in the respective surrounding (Revie and Uhlig, 2008). However, despite the exposed environment, metals are thermodynamically unstable and susceptible to getting corroded through a redox reaction with an oxidizing agent (Groysman, 2010). Oxidizing agents can be anything such as solvated protons, dissolved oxygen, water vapor, gases, acids, alkalis, etc. (Landolt, 2007).

$$\text{Metal} + \text{oxidizing agent} = \text{oxidized metal} + \text{reducing agent} \qquad (1.7)$$

Sulfuric acid is the most extensively used and produced chemical globally; every year, 200 million sulfuric acids are consumed. It is frequently utilized in the manufacturing of various chemicals, fertilizers, acid pickling, descaling, and metallic ore leaching (King, Davenport, and Moats, 2013). So, in this way, the sulfuric acid comes in contact with the mild steel materials.

1.4 Corrosion protection methods

Corrosion is indeed an irrevocable event and perhaps minimization or inhibition is the only solution to halt such catastrophes through various means such as electro-polishing (Hryniewicz, Rokosz, and Rokick, 2008), coatings (Voevodin *et al.*, 2003), and applications of inorganic and organic inhibitors (Breston, 1952). There are various methods presented in Table 1.1 by which the materials can be protected from the potential risk of corrosion in the respective environment.

Table 1.1: *Some corrosion protection methods*

S.N.	Methods	Specification (Fontana, 1986; Groysman, 2010; Roberge, 2008)
1.	Protective coatings	• Organic coating: paints, varnishes, lacquers, etc. • Inorganic coatings: glass, portland cement, and chemical conversion coatings. • Metallic coatings: electrodeposition, flame spraying, cladding, hot dipping, vapor deposition, etc.
2.	Electrochemical methods	• Anodic protection: application of anodic current • Cathodic protection: sacrificial and impressed current cathodic protection
3.	Material selection and design	• Selection: metals & alloys, metal purification, and application of polymeric materials • Design: Adjusting wall thickness and following design rules
4.	Corroding environment	• Changing mediums & concentrations, lowering temperatures, decreasing velocity, removing oxygen or oxidizers, employing inhibitors, etc.

1.5 Green Inhibitor

Inhibitors are chemical substances composed of organic to inorganic moieties, particularly for in-situ application that has a greater potential to suppress corrosion through the formation of protective layers in adequate quantities (Revie and Uhlig, 2008). Also, organic chemicals with heteroatomic centers are considered to have remarkable inhibitory efficacy (Sanyal, 1981). However, several synthetic inorganic and organic inhibitors were found to have harmful effects on both living beings and the environment during their production and use (Singh and Bockris, 1996). So, corrosion research is shaping toward green inhibitors by inventing compounds that are inexpensive, accessible, efficient, and environmentally safe to combat corrosion through more reliable approaches. toward green inhibitors by inventing corrosion inhibitors that are accessible, affordable, efficient, and environmentally friendly (Sastri, 2011). Green inhibitors are the type of corrosion inhibitor that is mostly plant-based natural products or biologically originated substances whose inhibition mechanism is based on the adsorption theory. Because the plants are rich in various primary and secondary metabolites which contain various complex heterocyclic aromatic

compounds with electron-rich heteroatomic centers (Sastri, 2011). However, the working efficiency of the green inhibitor gets affected by the operating temperature, time, structure, orientation, and concentration of the inhibitor molecule (*Thapa et al.*, 2022).

Currently, many researchers are studying various natural products such as essential oils, and plant extracts containing saponins, tannins, flavonoids, alkaloids, etc. obtained from the root, stem, leaf, fruit, and seeds as a green inhibitor to combat corrosion.

1.6 Significance of alkaloid in corrosion inhibition

Alkaloids generated from plants are being recognized as potent corrosion inhibitors in addition to other natural compounds (Fdil *et al.*, 2018; Karki *et al.*, 2022; Ngouné *et al.*, 2019; Palaniappan *et al.*, 2020). Alkaloids are allelochemical or secondary metabolite compounds made of basic nitrogen, sulfur, and oxygen atoms with electron-rich centers. As a result, they are strong candidates for green inhibitors (Babbar, 2015). They are naturally occurring organic bases containing large conjugated structures of non-bonding and π-electrons. Also, various families of alkaloids such as pyridine, indole, and purine-based alkaloids were found to be effective corrosion inhibitors for various metallic materials in numerous corrosive media (Verma *et al.*, 2019).

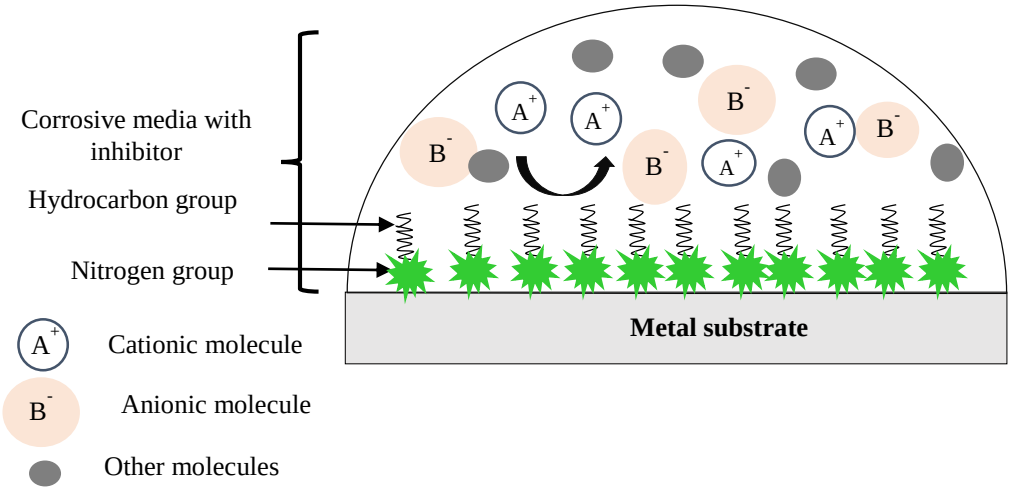

Figure 1.1: *Corrosion inhibition mechanism of alkaloid as a green corrosion inhibitor*

The general corrosion inhibition mechanism of alkaloids as a green inhibitor is illustrated in Figure 1.1. During the corrosion inhibition, the alkaloid molecules get adsorbed onto the surface. So, the nitrogen groups get accumulated on the metallic surface while the hydrocarbon chain gets aligned to the corrosive media containing the inhibitor. In this way, the material gets protected from corrosion (Bhattarai, 2010).

1.7 *Ageratina adenophora* (AA) as a corrosion inhibitor

The Asteraceae plant family includes the *Ageratina adenophora* Spreng., also known as *Eupatorium adenophorum*, which is a prominent, conspicuous, common, and foreign plant species that is believed to have originated in Mexico (Figure 1.2). The plant is more adaptable and more likely to reproduce in the invaded habitat by altering the microbial communities in the soil. This affects the soil, plants, and biodiversity (Wan *et al.*, 2010; Zhao *et al.*, 2019). According to the review of literature on the phytochemical (Thapa *et al.*, 2022), phytotoxicity (Zhou *et al.*, 2013), invasive nature, biological control (Poudel *et al.*, 2019), and pharmacological (Giri *et al.*, 2022) studies, the *Ageratina* is a plant that produces an abundance of both primary and secondary bioactive phytochemicals. Consequently, it is advantageous for pharmacological, antioxidant, anti-inflammatory, and bacterial applications. Moreover, the plant has medical history and is said to be harmful to some animals.

Taxonomic classification

Kingdom: Plantae

Division: Tracheophyta

Class: Magnoliopsida

Order: Asterales

Family: Asteraceae

Genus: *Ageratina*

Species: *adenophora* (Spreng.)

a) b)

Figure 1.2: *The vegetative parts of the Ageratina adenophora plant; a) flower and b) stem*

In a recent study, alkaloids were shown to be more abundant in *Ageratina* plant leaves than other bioactive substances including tannin, saponin, and flavonoids (Devkota and Das, 2022). It's interesting to note that the chemotaxonomic analysis of this plant's alkaloids also revealed the existence of Phosphorous with the functional groups P-O-C and P-O-P (Rosuman and Lirio, 2016). Among a group of heteroatoms (oxygen, nitrogen, sulfur, phosphorous), it is found that the phosphorous heteroatoms have the most efficient inhibitory efficiency (Chapagain *et al.*, 2022; Verma *et al.*, 2018). The plant subsequently becomes an appealing green inhibitor. *Ageratina adenophora*, however, hasn't been the subject of any studies as a green mild steel corrosion inhibitor

to date. Different pyrrolizidine alkaloids were reported in Genus *Ageratina*. The chemical structure of acetyl-lycopsamine (Becerra, 2013), 3-Hydroxy-2methyl-butyric acid-retronecinester, and lycopsamine (Setzer, 2018) is illustrated in Figure 1.3.

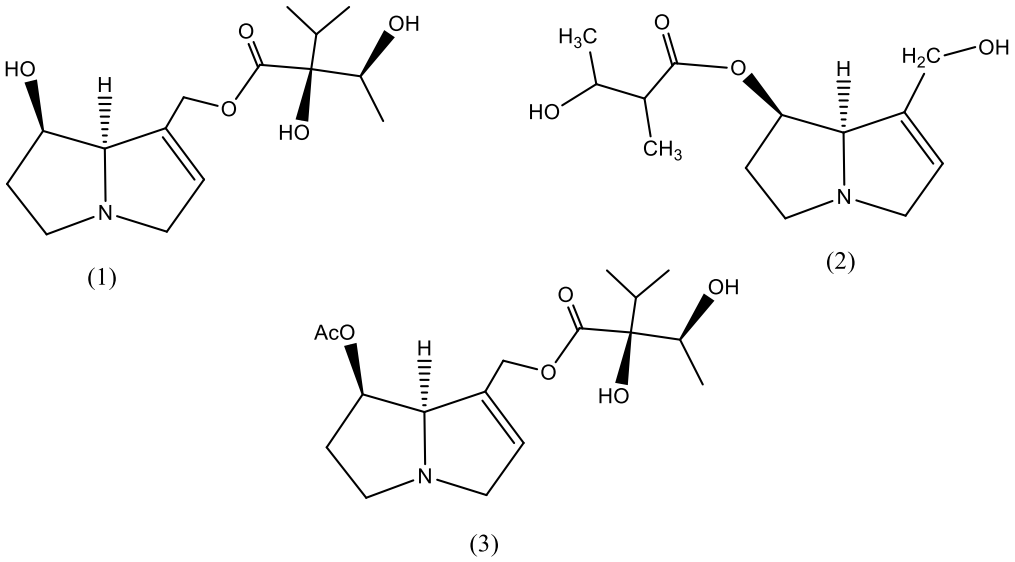

Figure 1.3: *The chemical structure of different alkaloids reported in the Ageratina adenophora plant; lycopsamine (1), 3-Hydroxy-2methyl-butyric acid-retronecinester (2), and acetyl-lycopsamine (3)*

1.8 Corrosion Monitoring Methods

The corrosion monitoring methods are the control methods for the rapid electrochemical corrosion investigations and corrosion rate characterizations of metal behavior under a particular environment. These methods are mostly based on the control of the physical properties of metal, the environment, and the border between metal-environment (i.e. physicochemical). Moreover, regardless of strong division, these techniques range from direct/intrusive to non-direct/non-intrusive techniques (Groysman, 2010). Some of the corrosion monitoring methods are described as follows.

1.8.1 Weight Loss Method

The weight loss method is the simplest direct physical corrosion monitoring method in which preliminary observation to examine the metal surface and corrosion products is possible to study the corrosion phenomenon and mechanism. The method has many benefits such as high reliability, and precision, and applies to a wide range of samples under different operating temperatures and pressure conditions (Groysman, 2010). In this method, resurfaced, initially weighed, and dimensioned mild steel samples are exposed to the corrosive media for a defined immersion period (Karki *et al.*, 2022).

From the weight loss measurements, the corrosion rate (CR), inhibition efficiency (IE%), and surface coverage (θ) can be calculated.

1.8.2 Potentiodynamic Polarization Measurement

The Potentiodynamic polarization measurements (PDP) is one of the corrosion rate measurement methods to study electrode kinetics of reaction rates at the interface based on the concepts of mixed-potential, tafel slope, corrosion current density, and exchange current density (Fontana, 1986; Revie and Uhlig, 2008). The polarization curve is an imitation of the corrosion behavior of metal as either anode or cathode (Groysman, 2010). In the experimental setup, the conventional three electrodes i.e., working electrode (metal under study), reference electrode, and counter electrode (for continuous current flow) are arranged in the electrochemical setup connected to the potentiostat (Revie and Uhlig, 2008). From the polarization data, the corrosion inhibition efficiency (IE%) can be calculated.

1.8.3 Electrochemical Impedance Spectroscopy (EIS)

Electrochemical impedance spectroscopy (EIS) is one of the most complex electrochemical steady-state techniques that measure the electric response of the interface region between the metal and environment to the applied low-amplitude AC signal over a certain frequency range (Groysman, 2010). The ability to use very small amplitude signals without appreciably affecting the parameters being examined is a key benefit of EIS over other electrochemical techniques (Roberge, 2008). So, from this method, the intrinsic material properties or specific processes of an electrochemical system's conductance, resistance, or capacitance can be easily studied regardless of the complexity of data interpretation (Magar, Hassan, and Mulchandani, 2021). In this study, a corrosion rate and the mechanism are studied from the recorded impedance as a function of frequency which represents the ability of the circuit to resist the movement of electric current. This method is best suited for studying general corrosion, evaluating protective coatings, assessing corrosion inhibitors, and much more (Groysman, 2010). From the obtained EIS data the corrosion inhibition efficiency can be calculated. The EIS results are mostly expressed in the following graphical plots;

I. Nyquist plot

The Nyquist plot is a type of graphical plot for analyzing the data obtained from electrochemical impedance spectroscopy. Here, the fitting of the imaginary part of impedance (Z_{imag}) in the ordinate and the real part of impedance (Z_{real}) in the

abscissa axis is used to analyze the resistive processes. When the MS surface comes in contact with an electrolytic solution an electrical double layer forms which is represented by a double-layer capacitance. Since, non-homogenous electrode surfaces make up a major portion of the real corrosion system the parameters of constant phase element (CPE) is applied in the defined frequency range (Magar *et al.*, 2021). It also has less calculation complexity compared to the bode plot (Huang *et al.*, 2016).

II. Bode plot

The Bode plot is a complex graphical plot as compared to Nyquist plot for analyzing the data obtained from the electrochemical impedance spectroscopy to study corrosion mechanism. The fitting of either magnitude as a function of frequency and phase angle of the impedance change as a function of frequency is used to calculate capacitance, CPE exponent (n), and CPE coefficient (Q) (Huang *et al.*, 2016; Magar *et al.*, 2021).

1.9 Objectives

1.9.1 General Objective

The general objective of this study is to extract alkaloids from the *Ageratina adenophora* stem and study its anticorrosion activity on MS samples in 1M H_2SO_4 solution.

1.9.2 Specific Objectives

The specific objectives of this study are as follows:

a) Extraction of alkaloids from the *Ageratina adenophora* stem and its chemical and spectroscopic characterization.
b) Study of corrosion inhibition efficiency of extracted alkaloids on MS by weight loss measurement method.
c) Electrochemical measurements and calculation of inhibition efficiency of inhibitor towards MS corrosion.
d) Study of adsorption isotherm and calculation of the thermodynamic parameters.

CHAPTER 2

LITERATURE REVIEW

An application of inhibitor to minimize corrosion of metallic material is a familiar concept (Groysman, 2010). Nowadays, emphasis is being paid to plant-derived alkaloids as efficient corrosion inhibitors because they are readily available, biodegradable, efficient, and environmentally friendly (Idouhli *et al.*, 2021). There are many research studies on alkaloids as green inhibitors for metallic corrosion in acidic media.

Faiz *et al.* studied the comparative inhibitory performance of dichloromethane crude extract and alkaloids obtained from the bark of the *Cryptocarya nigra* plant on the MS substrate in the 1 M HCl medium. They isolated three different alkaloids such as n-methylisococlaurine 1, N-methyllaurotetanine 2, and atherosperminine 3, through the cold percolation, maceration, and column chromatographic technique and characterized by the spectroscopic and microscopic techniques. Their results suggested a higher inhibition efficiency for dichloromethane crude extract than isolated alkaloids with a reduction in the oxygen reduction reaction (Faiz *et al.*, 2020). However, Idouhli et al. reported comparable inhibitory effectiveness of as-extracted alkaloids to the plant's crude extract when they studied different families of *Senecio anteuphorbium L.* plant as green inhibitors for steel corrosion in acidic media. They also concluded that alkaloids along with the terpenes are the major phytochemical components responsible for the synergistic effect of the overall crude extract (Idouhli *et al.*, 2021).

In another study, Ugi *et al.*, extracted secondary plant metabolites such as alkaloids, flavonoids, and saponins from the *Strongylodon macrobotrys* plant as a green inhibitor and studied their inhibition efficiency for MS corrosion in 0.2M NaCl medium. From the data obtained from the gravimetric and potentiodynamic polarization analysis, they reported the highest inhibition efficiency for the alkaloid extract with an almost nearly complete surface coverage of MS substrate compared to flavonoids and saponins extracts (Ugi *et al.*, 2020).

Hanini *et al.*, (2021) isolated alkaloids from the aerial parts of the gymnosperm plant *Taxus baccata* through surfactant-based extraction with the sonication methods and studied its anti-corrosion activity for carbon steel corrosion in 1M HCl for the first time. The quantum chemical calculations showed a lower E_{HOMO} value of Taxine B, and

higher electron donation ability, which is a suitable green alternative for the conventional corrosion inhibitors. Also, Shao *et al.* reported a new type of amide compound as a green inhibitor with an efficiency of 92.8% at 1 mM, which was extracted through the reflux method using alkaloid tryptamine and *Cinnamomum cassia presl* (Shao *et al.*, 2022)

Literature on the alkaloids extracted from the plants through various extraction routes as green inhibitors for metallic corrosion is presented in Table 2.1.

Table 2.1: *Alkaloids extracted from the plants as green inhibitors*

Plant/Part	Metal	Corrosive medium	Materials, methods, and findings	Ref.
Solanum xanthocarpum/ Stem	MS	1M H_2SO_4	• Extraction by cold percolation and solvent extraction techniques. • Tested parameters: weight loss, OCP, PDP, surface morphology, and adsorption isotherm. • Findings: 1000 ppm gave above 90% I.E. and can work up to 58 °C.	Thapa *et al.*, 2022
Coriaria nepalensis/Stem	MS	1M H_2SO_4	• Extraction by maceration and solvent extraction techniques. • Tested parameters were from the weight loss, PDP, and adsorption isotherm. • Findings: 1000 ppm gave IE above 90%.	Oli *et al.*, 2022
Cryptocarya nigra/Bark	MS	1M HCl	• Extraction by cold percolation, maceration, and column chromatography technique. • Anticorrosion activity was studied by the EIS and PDP methods. • Findings: 500 ppm plant dichloromethane crude extract gave 91.05% I.E. and 1000 ppm of the alkaloid (N-methyllaurotetanine 2) gave 88.05% I.E.	Faiz *et al.*, 2020
Acacia catechu/Bark	MS	1M H_2SO_4	• Extraction by cold percolation and solvent extraction techniques. • Parameters were studied from the weight loss, OCP, PDP, surface morphology, and adsorption isotherm. • Findings: 1000 ppm inhibitor solution gave above 93% IE.	Karki *et al.*, 2022
Taxus baccata/Aerial parts	Carbon steel	1M HCl	• Surfactant-based extraction with sonication • Quantum chemical computations, electrochemical methods (EIS and	Hanini *et al.*, 2021

			PDP), SEM, and weight loss parameters were investigated. • Findings: 200 ppm gave IE above 83%.	
Tabernaemontana contorta/Bark	C38 steel	1M HCl	• Extraction by maceration and column chromatography. • Used methods are EIS, PDP, spectroscopic solution analysis, and mass loss analysis. Findings: a) 16 mg/L gave 90% I.E. in both PDP and EIS tests. b) 8 mg/L is the optimum concentration of alkaloid.	Ngouné *et al.*, 2020
Rhynchostylis retusa	MS	1M H_2SO_4	• Extraction by cold percolation and solvent extraction techniques. • Used methods were weight loss, PDP, and optical imaging. • Findings: 1000 ppm achieved around 87% IE in weight loss and 93% IE in polarization, while 35 °C is the optimal temperature.	Chapagain *et al.*, 2022
Cinnamomum cassia presl	Q235 steel	0.5M HCl	• Extraction by reflux method. • EIS, PDP, surface analysis, computational methods, and the charge potential of zero charges were studied. • Findings: I.E. above 90 % were recorded the Inhibitor showed good stability up to 45 °C temperature.	Shao *et al.*, 2022
Rauvolfia macrophylla Stapf/Bark	C38 steel	1M HCl & 0.5M H_2SO_4	• Extraction by maceration, solvent extraction, and column chromatography. • Parameters such as EIS, temperature effect, PDP, and thermodynamic activation were studied. • Findings: a) Enhanced IE due to the introduction of additive 1mM Iodides. b) Inhibitor functioned as a cathodic inhibitor in H_2SO_4 and a mixed inhibitor in HCl. c) The inhibitor showed above 90% IE. d) Optimum inhibitor concentration was 100 mg/L and is stable up to the 60 °C.	Ngouné *et al.*, 2019
Strongylodon macrobotrys	MS	0.2 M NaCl	• Extraction by Soxhlet extractor extraction and solvent extraction methods. • Gravimetric, gasometric, EIS, PDP, and thermodynamic parameters were studied. • Findings: Alkaloid as an inhibitor gave the highest 99.2% IE.	Ugi *et al.*, 2020

All of the research work tabulated above largely followed the Langmuir adsorption isotherm. Also, the commercialization of green inhibitors for metallic corrosion is the purpose of all of these scientific studies. Besides these reported plants, there are many other potential plants, which can be executed for the application against the corrosion of materials like mild steel. To the best of our knowledge, the methanolic extract of *Ageratina adenophora* has not been reported to be used for the inhibition of green corrosion in mild steel in acidic media.

CHAPTER 3

MATERIALS AND METHODS

3.1 Collection of Plant Material and Preparation of Powder

The stems of *Ageratina adenophora* (AA) were collected from Dang, Ghorahi (Latitude: 28.05775° N, Longitude: 82.48603° E, and Elevation: 2,300 feet/700 m), in September 2022. The geographical location of the sample collected area is shown in Figure 3.1. The collected plant materials were then shade-dried and ground into a fine powder using a grinding machine.

Figure 3.1: *Google map of the plant collected area*

3.2 Alkaloid Extraction

About one hundred grams of the powdered plant materials were immersed in 750 mL of methanol solution for one week. Meanwhile, after every 24 hours, a glass rod was used to stir the immersed sample. After one week the immersed sample was filtered to obtain filtrate in a beaker while the residue was discarded. The filtrate was then acidified with 5% tartaric acid until the pH reached 2.80. As a result, precipitation of the alkaloids in salt was produced and left overnight to decant. It was then filtered and the residue was dissolved in aqueous ammonia solution. The prepared alkaline solution was then subjected to solvent extraction in a 1:1 ratio of dichloromethane (DCM): alkaline solution (Thapa *et al.*, 2022).

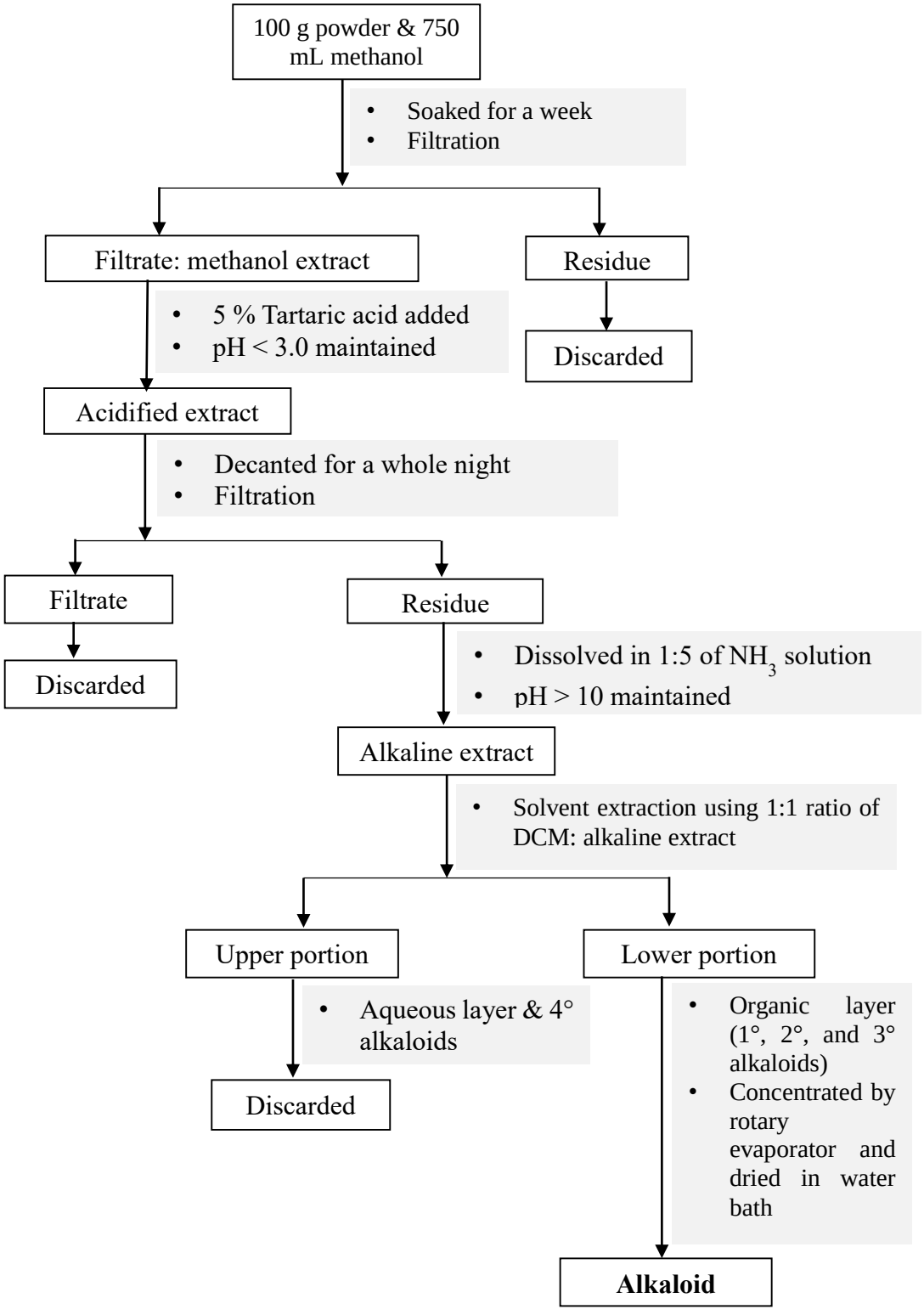

Figure 3.2: *Flow chart showing several steps involving extraction of alkaloids*

In the separating funnel, the upper portion contains an aqueous layer while the lower portion contains alkaloids separated by the DCM layer which were collected in a beaker. The organic material was subsequently concentrated using a rotary evaporator,

and dried by using a Clifton water bath at 40° C. The dry mass is labeled as *Ageretina adenophora* alkaloid (AA). The detailed process of extraction is shown in Figure 3.2.

3.3 Preparation of Corrosive Media

An appropriate volume of 55.12 mL of commercial concentrated sulfuric acid (Fisher Scientific, 97%, sp. gr. 1.835) was used for making 1 M H_2SO_4 solution in a 1000 mL volumetric flask containing distilled water. Then it was diluted up to a mark followed by standardization with 2 M NaOH solution. This was taken as corrosive media as well as a solvent medium for preparing inhibitor solutions.

3.4 Preparation of Inhibitor Solution

One gram of dried alkaloid was dissolved in a small volume of methanol (Thermo Fischer Scientific, 99% sp. gr. 0.791) in a 1000 mL of volumetric flask and diluted up to the mark by using 1 M H_2SO_4. 1000 ppm of inhibitor solution is the final stock solution. From the dilution method, this stock solution was used to prepare a series of inhibitor solutions in various concentrations (i.e. 200, 400, 600, and 800 ppm respectively).

3.5 Preparation of Mild Steel Specimen

The mild steel (MS) sample coupons were bought from the neighborhood shop in Sukedhara, Kathmandu. Then, different grits of silicon carbide paper in the range of 80 to 1000 were used to polish each coupon. Each MS coupon was sonicated in ethanol for 10-15 minutes, and dried. Furthermore, the dimensions (length, breadth, and height) of each MS coupon were measured using digital Vernier calipers. This process of pretreatment was repeated before each weight loss and electrochemical experiment.

3.6 Qualitative Tests for Alkaloids

The preliminary tests of as-prepared alkaloids were carried out through chemical and spectroscopic analysis.

3.6.1 Chemical Analysis

The chemical identification of as-prepared alkaloids was carried out using three different chemical tests: Mayer's, Dragendorff's, and Wagner's which can be summarized as follows:

a) Mayer's Test

A freshly prepared Mayer's reagent was used for a qualitative chemical test of alkaloids which was prepared by dissolving 1.36 g of $HgCl_2$ and 5 g of KI in 100 mL of distilled

water. The addition of a few drops of Mayer's reagent to 2 mL of alkaloid solution produces an orange precipitate of potassium-alkaloid. This confirms the presence of an alkaloid.

b) Dragendorff's Test

The Dragendorff's reagents were prepared in the following steps:

a) Preparation of Solution A: 3 g of Bismuth nitrate was slowly dissolved in 4 N H_2SO_4 (8 mL).
b) Preparation of Solution B: 12 g of KI was dissolved in 18 mL of distilled water.
c) Dragendorff's reagent: Both Solution A and B were mixed in a 50 mL volumetric flask containing distilled water.

The addition of a few drops of Dragendorff's reagent to 2 mL of alkaloid solution produces an orange-red precipitate of potassium-alkaloid. This confirms the presence of an alkaloid.

c) Wagner's Test

For the Wagner's reagent, 2 g of iodine was mixed with 6 g of KI in 100 mL of distilled water. The addition of a few drops of Wagner's reagent to 2 mL of alkaloid solution produces a reddish-brown precipitate of potassium-alkaloid. This confirms the presence of an alkaloid.

3.6.2 Spectroscopic Analysis

The molecular identification, characterization, and analysis of the as-prepared alkaloids (AA) was carried out through the following two spectroscopic methods.

a) UV-Vis Spectroscopic Analysis

A 5 ppm methanolic solution of AA was prepared. The spectrum was then recorded in the 200-800 nm wavelength range using a UV spectrophotometer (Labtronics, LT-2802) at Amrit Campus in Kathmandu with a scanning interval of 1 nm.

b) Fourier Transform Infra-red (FTIR) Spectroscopic Analysis

FTIR spectroscopy is an important tool for functional group identification and determination. The FTIR spectra of alkaloid, polished mild steel, and MS surface after 1 h immersion in an inhibitor solution were recorded in the Perkin-Elmer Spectrum IR version 10.6.2 between the wave number range of 450-4000 cm^{-1} with a resolution of 4 cm^{-1}. Also, an isopropanol solvent was employed for the background correction before each experiment in spectroscopy.

3.7 Weight Loss Measurement Method

The weight loss measurement is one of the direct corrosion monitoring methods to study the steady-state corrosion rate in metals (Atrens *et al.*, 2022). In this method, initially, pretreated and weighed mild steel specimens were immersed in the acid with and without different concentrations of inhibitor solutions for varying intervals of time. The immersion times were 0.5, 1, 3, 6, 9, 18, and 24 h respectively. Afterward, the MS samples were taken out, washed, dried, and reweighed using an analytical weighing balance (Phoenix, PH2204C). Similarly, the effect of immersion time and inhibitor concentration on the metallic substrate was investigated from the acquired data. Also, the effect of temperature was studied for an hour immersion time at 28, 38, and 48 °C respectively. The corrosion kinetics, thermodynamic parameters, and adsorption isotherms were studied from the obtained data. The corrosion rate (CR), inhibition efficiency (IE%), and surface coverage (θ) were then computed from the equations (1.8), (1.9), and (2.0).

$$\text{Corrosion Rate (CR)} = \frac{K \times \Delta W}{A \times T \times D} \quad (1.8)$$

$$\text{Inhibition efficiency (IE\%)} = \frac{w_a - w_p}{w_a} \times 100 \quad (1.9)$$

$$\text{Surface coverage } (\theta) = \frac{w_a - w_p}{w_a} \quad (2.0)$$

Where,

K = corrosion rate constant = 87600

ΔW = weight loss in gram

A = surface area of MS in cm^2

T = immersion time in an hour

D = density of MS in g/cm^3

Wa = weight loss of MS in acid and different concentrations of inhibitor solutions

Wp = weight loss of MS in acid and different concentrations of inhibitor solutions

3.8 Electrochemical Measurement Methods

Electrochemical tests were carried out using Potentiostat (Gamry Interface 1010B Potentiostat/Galvanostat, run by Gamry Framework 7.9.0 analyst version) at the Central Department of Chemistry, Tribhuvan University, Kathmandu, Nepal. By using

MS as the working electrode, platinum (Pt) as the counter electrode, and saturated calomel electrode (SCE) as the reference electrode, a conventional three-electrode electrochemical setup was formed. The pretreated MS coupons were submerged for an hour in corrosive medium and inhibitor solutions as electrolytes. The electrochemical apparatus was then placed inside the CHI picoamp booster and Faraday cage. Which helped in avoiding electrical interference and frequency noise during analysis. As the potentiostatic EIS is a non-destructive electroanalytical method, it was performed before the PDP analysis for all MS samples in as-immersed and one-hour immersed conditions.

Before every EIS analysis, a 99-second open circuit delay was implemented. Then, using an AC voltage of 10 mV rms at a scan rate of 5 points per decade, the EIS curve was recorded subsequently between the 100 kHz to 0.01 Hz frequency range. Then after analyzing the obtained data, the inhibition efficiency was determined from equation (2.1).

$$\text{Inhibition efficiency (IE)} = \left(1 - \frac{R_{ct}}{R_{ct(inh)}}\right) \times 100 \qquad (2.1)$$

Where,

R_{ct} = Charge transfer resistance of the MS samples in the 1M H_2SO_4 solution expressed in Ωcm^2

$R_{ct(inh)}$ = Charge transfer resistance of the MS samples in the inhibitor solution expressed in Ωcm^2.

The polarization curves have been recorded by scanning at a rate of 1 mV/s in the potential range between -0.8 to -0.2 V vs SCE. From equation (2.2) the inhibitory efficiency (IE) was calculated.

$$\text{Inhibition efficiency (IE\%)} = \left(1 - \frac{I_{corr\ (inh)}}{I_{corr}}\right) \times 100 \qquad (2.2)$$

Where,

I_{corr} = Corrosion current density of the MS samples in 1M H_2SO_4 solution expressed in Acm^{-2}

I_{corr} = Corrosion current density of the MS samples in the inhibitor solution expressed in Acm^{-2}.

CHAPTER 4

RESULTS AND DISCUSSION

4.1 Characterization of as-prepared alkaloids

Alkaloids were successfully separated from the stems of the *Ageratina adenophora* plant using extraction methods such as cold percolation and solvent extraction techniques. For the confirmation of the as-prepared alkaloids, spectroscopic analysis and qualitative chemical tests were carried out.

4.1.1 Qualitative chemical tests

The observation and results of each qualitative chemical test of as-prepared alkaloids are presented in Table 4.1. Various pyrrolizidine molecules as major alkaloids are present in this plant. So, in this study, lycopsamine as a reference alkaloid molecule has been used to illustrate the reactions between the alkaloid and the three different chemical reagents (Chapagain, 2022) which are described as follows:

Table 4.1: *Qualitative chemical tests for as-prepared alkaloids*

Modes	**Mayer 's Test**	**Dragendorff 's Test**	**Wagner 's Test**
Observation			
Precipitate	Orange	Orange-red	Reddish brown
Inference	Positive	Positive	Positive
Result	Alkaloids presence	Alkaloids presence	Alkaloids presence

a) Mayer's test

The freshly prepared potassium mercuric iodide $K_2[HgI_4]$ is Mayer's reagent. The addition of a few drops of Mayer's reagent to the alkaloid solution formed an orange precipitate of potassium-alkaloid thus indicating the presence of alkaloids. The possible involved reaction concerning the lycopsamine molecule is given below.

$$HgCl_2 + 2KI = HgI_2 + KCl$$

$$HgI_2 + 2KI = K_2[HgI_4]$$

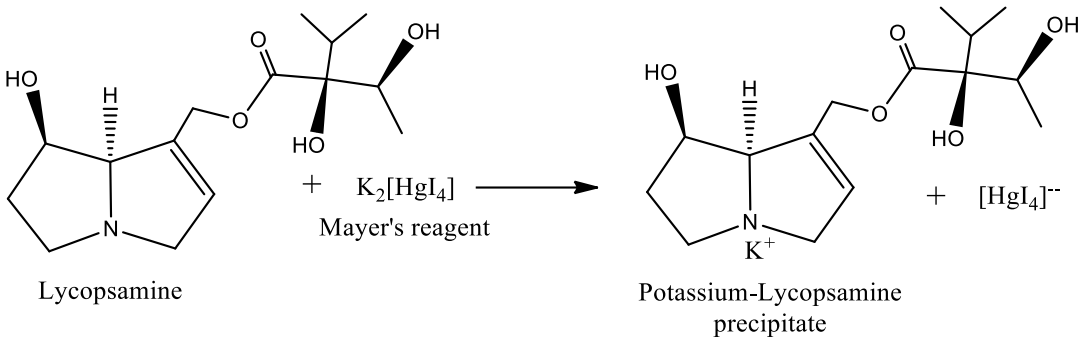

Lycopsamine

Potassium-Lycopsamine precipitate

b) Dragendorff's test

The addition of a few drops of Dragendorff's reagent (i.e. Potassium bismuth iodide) to the alkaloid solution formed an orange-red precipitate of potassium-alkaloid thus indicating the presence of alkaloids. The possible involved reaction concerning the lycopsamine molecule is given below.

$$Bi(NO_3)_3 + 3KI = BiI_3\ (Brown) + 3KNO_3$$

$$BiI_3 + KI = K[BiI_4]$$

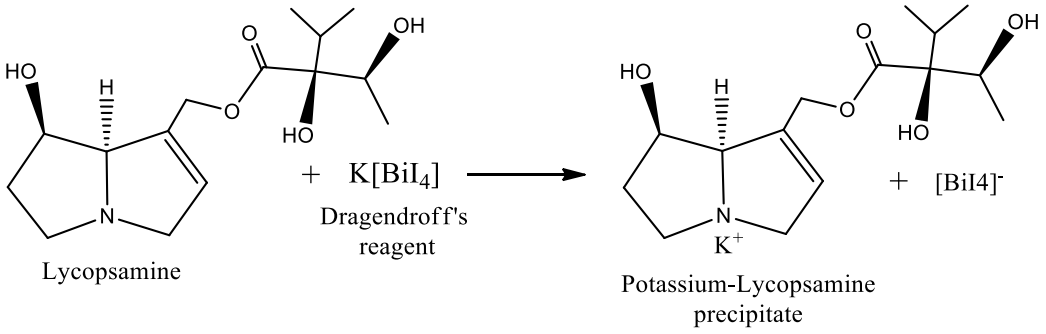

Lycopsamine

Potassium-Lycopsamine precipitate

c) Wagner's test

The potassium and tri-iodide ions in the solution are obtained by dissolving iodine molecules in the potassium iodide solution. The interaction of these ions with the alkaloids produces a reddish-brown precipitate of potassium alkaloid thus indicating the presence of alkaloids. The possible involved reaction concerning the lycopsamine molecule is given below.

$$I_2 + I^- = I_3^-$$

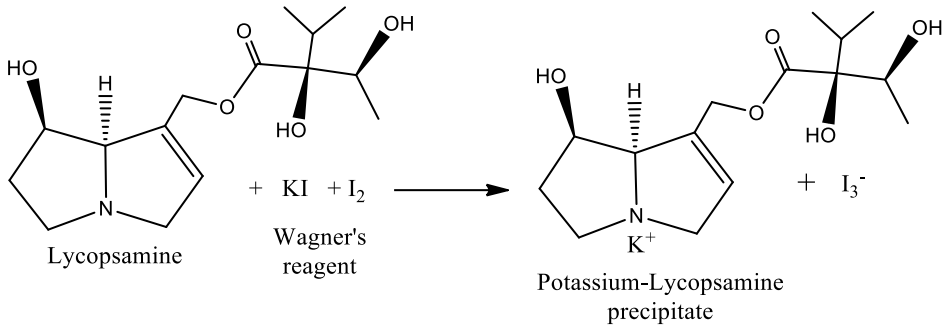

4.1.2 Spectroscopic analysis

a) UV-Vis Spectroscopic analysis

When the as-prepared alkaloid was exposed to UV or visible light, it exhibited spectra with a broad peak at 305 nm which is shown in Figure 4.1. This is due to the n-π* electronic transition, thus suggesting the presence of an unsaturated molecule or a lone pair of electrons (Oli *et al.*, 2022; Silverstein & Webster, 2005). If lycopsamine is used as a reference alkaloid molecule, then this peak confirms the presence of an aromatic ring with heteroatom nitrogen and a polyphenolic group.

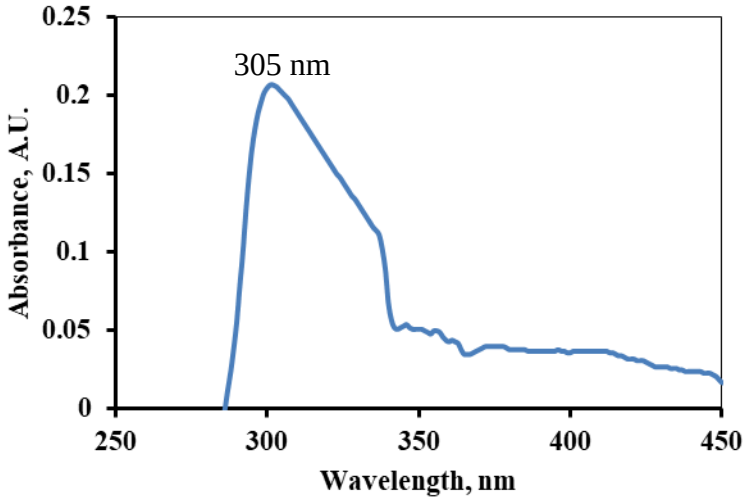

Figure 4.1: *The UV-Vis spectrum of as-prepared alkaloids of Ageratina adenophora (AA)*

b) FTIR Spectroscopic analysis

The Fourier Transform Infrared Spectroscopic measurements were carried out on the freshly gritted MS coupons, pure alkaloid, and on the MS surface which was submerged for one hour in a 600 ppm inhibitor solution. The collected spectral data were then compiled in a graphical plot to observe and study the adsorption of alkaloid molecules on the MS sample which is illustrated in Figure 4.2. In the graph, in the range of 3469-3272 cm^{-1}, the inhibitor exhibited a large peak at 3385 cm^{-1}. It corresponds to the

stretching vibrations of N-H and O-H of primary amine and hydroxyl functional groups. The stretching vibrations of C-H by the asymmetric aliphatic hydrocarbon group, there is an additional sharp peak at 2925 and 2859 cm^{-1}. Also, there are another two sharp peaks at 1717 and 1663 cm^{-1} which is due to the stretching vibrations of symmetric and asymmetric carbonyl groups (C=O). Likewise, the acute peaks at 1459 and 1374 cm^{-1} are associated with the bending vibrations of the carboxylic acid and C-H of the aldehydic group. There were many peaks in the 1240–1064 cm^{-1} range, one of which was extended and attributed to the C–N stretching vibrations at 1064 cm^{-1} (Silverstein & Webster, 2005). Additionally, a tiny sharp peak that occurred at 977 cm-1 may be related to the P-O-P or C-N-C group (Yu *et al.*, 2020). Nevertheless, there is neither a broad peak around 700 cm^{-1} nor a sharp peak in the 1050–970 cm^{-1} range. This ensures the presence of the C-N-C group and the absence of the P-O-P group (Silverstein & Webster, 2005).

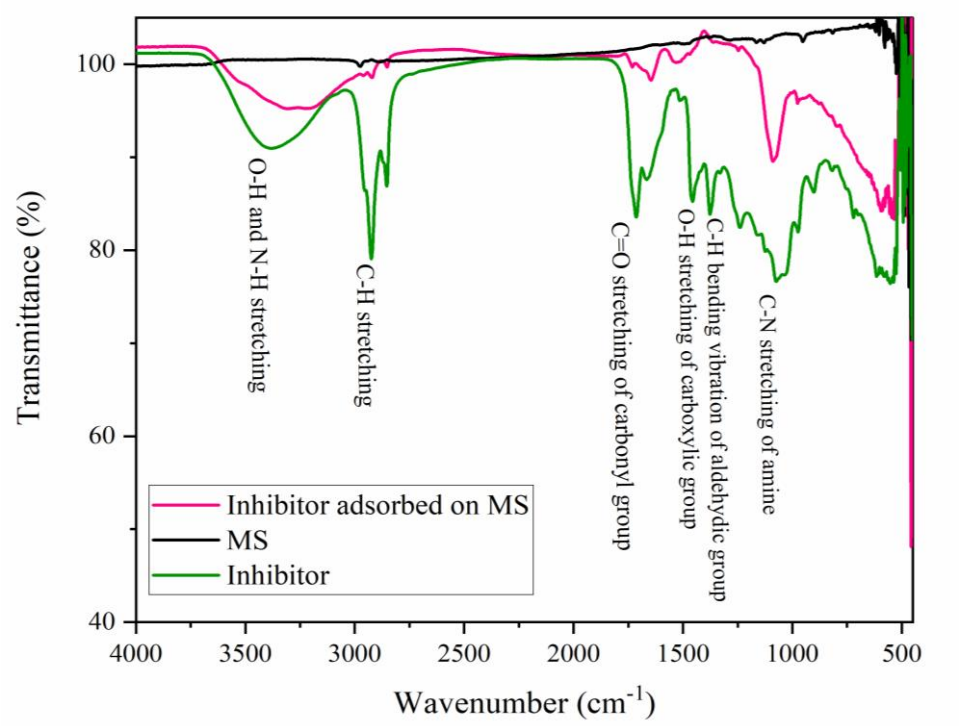

Figure 4.2: *Combined FTIR spectra of MS and inhibitor molecules on the FTIR spectrum of MS submerged in a 600 ppm inhibitor solution for one hour.*

A wide peak in the 3397-3288 cm^{-1} was observed in the FTIR spectrum of the inhibitor adsorbed on the MS substrate, which suggested that the O-H and N-H groups of the alkaloid molecules had adhered to the MS substrate. The absorption band at 1645 and 1084 cm^{-1} also showed that the C=O and C-N groups were adsorbing on the surface.

However, on the polished MS surface, there aren't any notable peaks. This reveals the formation of a thin layer of alkaloids on the MS surface (Karki *et al.*, 2022). This is due to the interaction between the functional groups such as C=O, N-H, O-H, and C-N, with vacant d-orbitals of MS.

4.2 Weight Loss Measurements

4.2.1 Effect of Immersion Time

Figure 4.3 in general illustrates a distinct variation in weight loss per unit area of MS sample subjected to acid with and without inhibitor solution for the designated immersion time which in turn leads to an elevated corrosion rate with the reduction in the inhibition efficiency of alkaloid molecules. In this experiment, the MS coupon immersed in the acidic solution clearly showed a greater weight loss than the corresponding sample immersed in the inhibitor solution throughout the entire immersion time. In terms of weight loss per unit area the MS specimens followed a successive order of acid > 200 ppm > 400 ppm > 600 ppm > 800 ppm (Figure 4.3a). On the one hand, the weight loss for MS substrate immersed in an acid solution for 18 hours was 0.0678 g/cm^2 while on the other hand, it was 0.0052 g/cm^2 for the corresponding sample in 800 ppm for the same timeframe as presented in Table 4.2. The inhibitor causes a weight loss differential of 0.0626 units. This occurs as a result of the buildup of adsorptive layers that obscured the reactive metal ions from the corrosive environment, reducing weight loss from the substrate and boosting the effectiveness of inhibition (Chapagain *et al.*, 2022; Karki *et al.*, 2022).

Table 4.2: *The weight loss (g/cm^2) of the MS sample immersed in different concentrations of inhibitors for different immersion times*

Time (h)	Acid	200 ppm	400 ppm	600 ppm	800 ppm
0.5	0.003140	0.000332	9.97E-05	0.000103	2.47E-05
1	0.006784	0.001022	0.000634	0.000476	0.000206
3	0.016639	0.004712	0.002530	0.001781	0.001244
6	0.025999	0.008120	0.004291	0.002632	0.002098
9	0.043782	0.014668	0.006776	0.004182	0.002564
18	0.067848	0.026551	0.016421	0.008626	0.005211
24	0.080207	0.047405	0.032196	0.028718	0.017744

Figure 4.3a illustrates the effect of the designated immersion period on the weight loss of MS samples dipped in acid with and without inhibitor concentrations. While Figure

4.3b depicts its effect on the inhibition efficiency of different inhibitor concentrations for MS corrosion in 1 M H_2SO_4 solution given below.

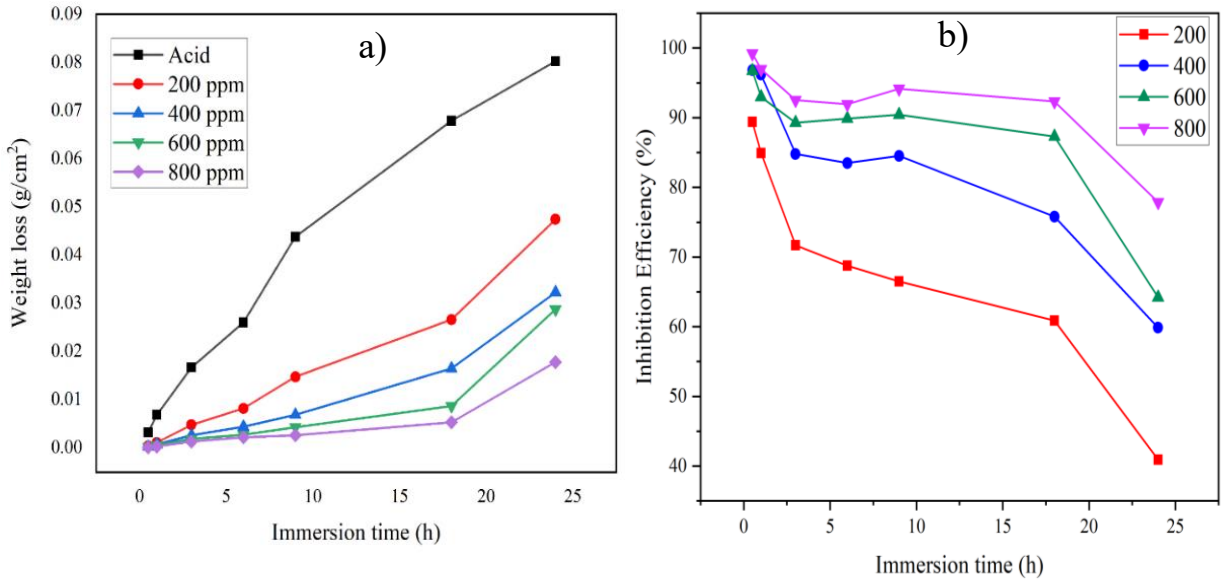

Figure 4.3: *The effect of immersion time on a) the weight loss of MS sample immersed in acid with and without inhibitor concentration and b) inhibition efficiency of various inhibitor concentrations for MS in 1 M H_2SO_4 solution*

The abrupt decrement in both weight loss and inhibition efficiency occurred with the increment in the designated immersion time (Figure 4.3), this may be explained by the following two reasons. The initial reason might be related to the instantaneous removal of the inhibitor molecule from the sample surface through the desorption process, causing a rapid disintegration in the exposed area (Thapa *et al.*, 2022). The second reason is related to the structural features of inhibitor molecules which is their size, orientation, and the nature of interaction that leads to a certain type of abnormalities on the inhibitor layer (Chapagain *et al.*, 2022).

4.2.2 Effect of Inhibitor Concentration

The effectiveness of alkaloids in protecting metal in corrosive conditions is primarily dependent on the concentration employed (Chapagain *et al.*, 2022; Faiz *et al.*, 2020). It was observed that the alkaloid's inhibitory efficiency enhanced with an increase in concentrations in a sequence of 200 ppm < 400 ppm < 600 ppm < 800 ppm respectively as shown in Table 4.3. The 800 ppm inhibitor solution exhibited the highest inhibitory performance of 96.95% while the 200 ppm inhibitor solution revealed a relatively small amount of inhibition of 84.93% after one hour of immersion. The abundance of alkaloid molecules for the almost complete surface coverage may be the reason behind the

maximum inhibitory performance while the minimum inhibitory action may be due to the insufficient number of alkaloid molecules in the corrosive media. Except for the 200 ppm inhibitor solution, 18 hours was the longest immersion period during which significant efficiency of above 70% was found. The inhibitory efficiency of the 800 ppm solution, however, decreased to 77.88% after 24 hours, while for the 200 ppm inhibitor solution, the I.E. declined to 40.89% as displayed in Figure 4.4. Such decline is due to the insufficient inhibitor molecules to protect the MS surface thus enabling the corrosive attack from the acid (Oli *et al.*, 2022).

Table 4.3: *The I.E. (%) of different concentrations of inhibitor for MS corrosion in 1M H_2SO_4*

Time (h)	200 ppm	400 ppm	600 ppm	800 ppm
0.5	89.39	96.82	96.71	99.21
1	84.93	96.19	92.97	96.95
3	71.68	84.79	89.29	92.52
6	68.77	83.49	89.87	91.93
9	66.49	84.52	90.44	94.14
18	60.87	75.79	87.28	92.32
24	40.89	59.86	64.19	77.88

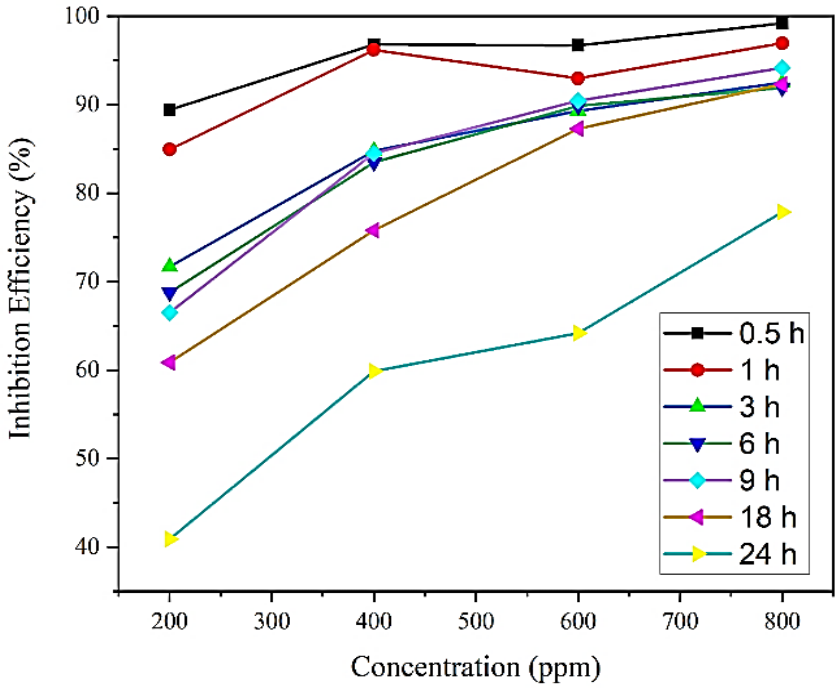

Figure 4.4: *Effect of various concentrations of alkaloid on the inhibitory action for MS corrosion in 1M H_2SO_4*

4.2.3 Effect of Temperature

Besides the structure, molecular vibration, and concentrations of the alkaloids, the operating temperature also influenced the inhibitory performance of the inhibitor solution (Thapa *et al.*, 2022). In this study, a variation in the weight loss of MS sample in acid with and without the presence of an inhibitor along with the variation in the inhibition efficiency of the alkaloid was observed with the increase in temperature between 28-48° C. The effect of temperature on the weight loss (g/cm^2) of the MS sample immersed in acid and different concentrations of inhibitors for 1 h immersion is presented in Table 4.4. At room temperature of 28° C, the MS sample in the inhibitor solution implicitly lost weight while at the 38 °C, the weight loss of MS in both acid and 200 ppm inhibitor solution was nearly identical. The quick removal of inhibitor molecules from the substrate may be the reason behind this. In contrast to the other inhibitors (i.e., 400 and 600 ppm), the sample in the 800 ppm inhibitor solution showed minimal weight loss.

Table 4.4: *The effect of temperature on the weight loss (g/cm^2) of the MS sample immersed in acid and different concentrations of inhibitors for 1 h immersion*

Temperature (°C)	Acid	200 ppm	400 ppm	600 ppm	800 ppm
28	0.006785	0.001022	0.000634	0.000476	0.000206
38	0.011647	0.007832	0.005206	0.004149	0.002535
48	0.022757	0.014556	0.010719	0.007852	0.006525

Table 4.5 displays the influence of temperature on the effectiveness of different inhibitor concentrations in suppressing MS corrosion during one-hour immersion in corrosive media. From the tabulated data, a 20-50% decrease in inhibition efficiency at the temperature range between 28-38 °C was observed. About a 1-8% drop in the inhibition efficiency for the temperature up to 48 °C was seen after that. This suggests that either 28 or 48° C is the optimum temperature for the formation of the inhibitor layer.

Table 4.5: *The effect of temperature on I.E. (%) of different concentrations of inhibitor for MS corrosion in 1M H_2SO_4 for 1 h immersion*

Temperature (°C)	200 ppm	400 ppm	600 ppm	800 ppm
28	84.92	96.18	92.97	96.95
38	32.75	55.30	64.37	78.23
48	36.03	52.89	65.49	71.32

Based on the recorded data (From tables 4.4 and 4.5), a graphical plot of the weight loss of the MS sample against the temperature and the inhibition efficiency of the different concentrations of the inhibitor against the temperature is illustrated below in Figures 4.5 a) and b), respectively.

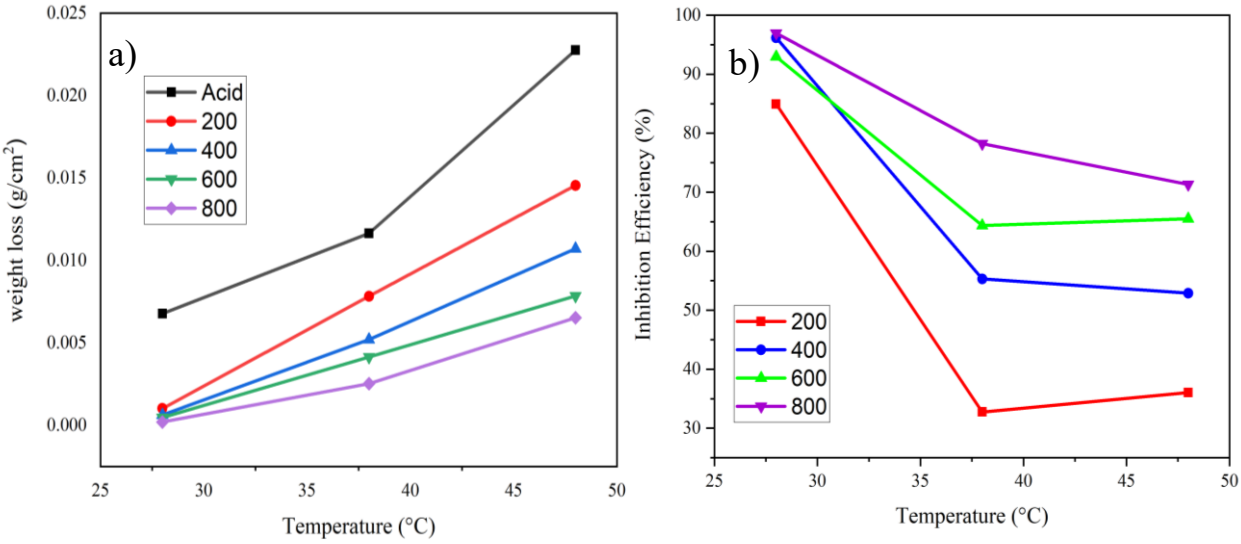

Figure 4.5: *Temperature effect on the b) weight loss of MS samples in acid with and without inhibitor concentration and a) on the inhibitory performance of different concentrations of inhibitor for 1 h immersion*

In Figure 4.5a, the MS in 200 ppm inhibitor has shown a weight loss curve near the weight loss curve of the sample in acid at 38 °C due to the quick dissociation of inhibitor molecules from the surface. As a result, the 200 ppm inhibitor solution displayed a significant nonlinearity in Figure 4.5b while in the case of 800 ppm inhibitor, this is less pronounced. Nonetheless, linearity in the curve was seen for samples with inhibitor concentrations of 400, 600, and 800 ppm between 38 to 48 °C, as depicted in Figure 4.5b.

The alkaloid's ability to inhibit is mainly carried on by physisorption, subsequently followed by chemisorption, which is linked to the molecular vibrations (Chapagain *et*

al., 2022) and since molecular vibrations are amplified at high temperatures, temperature-induced physical dissociation from the MS substrate is therefore possible.

4.3 Adsorption Isotherm

Adsorption isotherm models are crucial visual graphs for comprehending the basic characteristics of how organic molecules adsorb on surfaces like mild steel (Oli *et al.*, 2021; Wang & Guo, 2020). It was proposed by Karki *et al.* that there is always an equal probability for the concurrent adsorption and substitution between the water and inhibitor/alkaloid molecules on the surface of the MS when the alkaloid was dissolved in an acid solution to prepare the inhibitor solution (Karki *et al.*, 2022). In this experiment, three different models i.e., Langmuir, Freundlich, and Temkin adsorption isotherms were tested to study the adsorption phenomena, and corrosion inhibition mechanism, and to determine Gibb's free energy of adsorption. Also, the molar concentration (C) of the inhibitor solution was computed using the molecular weight of the lycopsamine alkaloid as a reference molecule.

4.3.1 Langmuir Adsorption Isotherm Model

The Langmuir model is an important isotherm model to study the adsorption of corrosion inhibitors (Ituen *et al.*, 2017). The equation (2.3) is the Langmuir adsorption isotherm equation which is employed to fit a graphical plot using $\frac{C_{inh}}{\theta}$ against C_{inh} (mol/L) as shown in Figure 4.6 below.

$$\frac{C_{inh}}{\theta} = \frac{1}{K_{ads}} + C_{inh} \tag{2.3}$$

Where,

C_{inh} = inhibitor's concentrations expressed in $molL^{-1}$ and θ = surface coverage of MS

K_{ads}= Langmuir adsorption equilibrium constant

The Gibbs free energy of the adsorption (ΔG_{ads}) was calculated from the K_{ads} from equation (2.4).

$$\Delta G_{ads} = -RT \ln K_{ads} \tag{2.4}$$

Where R is the ideal gas constant ($Jmol^{-1}K^{-1}$).

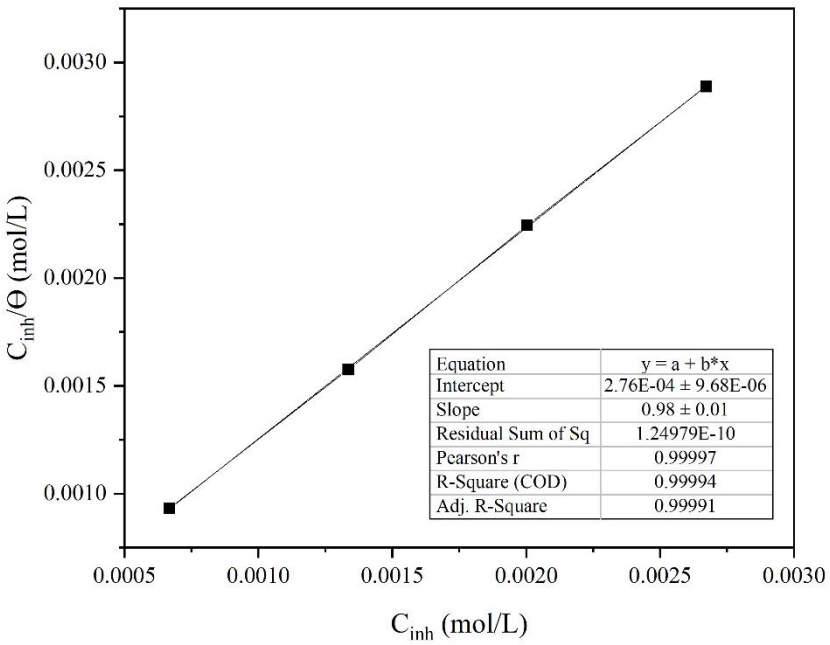

Figure 4.6: *Langmuir adsorption isotherm plots for the MS in 1 M H_2SO_4 with the different concentrations of inhibitor*

From the graphical plot, a straight line with a regression coefficient (R^2) of nearly one was found. This indicates that the monolayers first form on equivalent adsorption sites before multilayers. At 301 K, the computed values for the free energy of adsorption and adsorption equilibrium are -30.35 kJ mol^{-1} and 3333.33 L mol^{-1}, respectively. The free energy value (ΔG_{ads}) is found to be less than 40 kJ mol^{-1} but greater than 20 kJ mol^{-1}. According to Chapagain *et al.*, this suggests an insignificant electrostatic interaction in conjunction with a chemical interaction between lone pairs of electrons at the electronegative sites of inhibitor molecules and the MS sample (Chapagain *et al.*, 2022; Karki *et al.*, 2018), resulting in the formation of a thin barrier on the MS junction.

4.3.2 Freundlich Adsorption Isotherm Model

The Freundlich adsorption isotherm model was tested by using an equation (2.5) in which the value of "n" is used to determine the spontaneity and the nature of the adsorption (Toor & Jin, 2012). The fitting of the Freundlich isotherm was performed by plotting ln θ on the ordinate and ln C_{inh} on the abscissa axis as illustrated in Figure 4.7.

$$\ln \theta = \ln K + \frac{1}{n} \ln C_{inh} \tag{2.5}$$

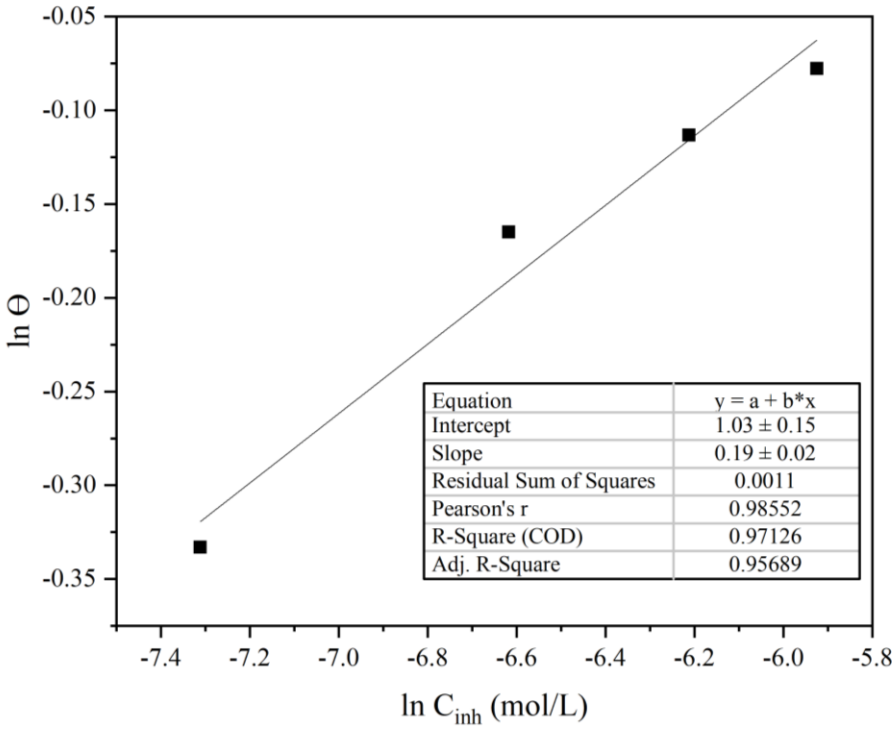

Figure 4.7: *Freundlich adsorption isotherm plots for the MS in 1 M H_2SO_4 with the different concentrations of inhibitor*

The graphical plot shown in Figure 4.7 gave a straight line with a slope value (1/n) of 0.1852 and a regression coefficient value (R^2) of 0.971which is in the barely acceptable range. Since the obtained value of 1/n is situated from 0 to 1 this suggested a spontaneous adsorption process (Karki *et al.*, 2022). However, the R^2 value is merely near to unity the adsorption does not follow this isotherm model.

4.3.3 Temkin Adsorption Isotherm Model

The Temkin adsorption equation (2.6) was used to study the corrosion inhibition mechanism and interaction nature. The Temkin plot was fitted by plotting the θ on the y-axis against ln C_{inh} on the x-axis. This produces a slope of a straight line with an R^2 coefficient value of 0.981 which is near to the unity as shown in Figure 4.8.

$$\theta = -\frac{1}{2a}\ln C_{inh} - \frac{1}{2a}\ln K \qquad (2.6)$$

Where "**a"** is an interaction parameter.

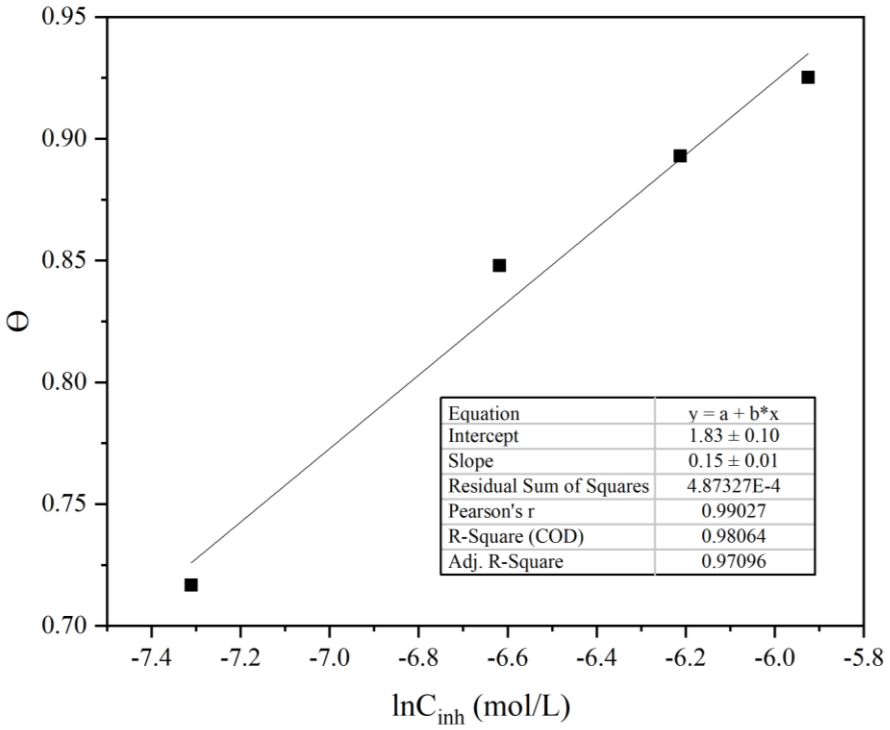

Figure 4.8: *Temkin adsorption isotherm plots for the MS in 1 M H_2SO_4 with the different concentrations of inhibitor*

The recorded R^2 value, however, was slightly lesser than the recorded R^2 value seen in the Langmuir model, confirming that the Langmuir model is strongly obeyed when an inhibitor gets adsorbed onto the MS surface. The computed values of the interaction parameters (a) and K were found to be negative 3.31 and 181,679.60 respectively. This indicates the significant adsorption and adhesion of the inhibitor compounds to the MS surface (Karki *et al.*, 2022; Tan *et al.*, 2021). The calculated parameters of three different isotherm models are tabulated in Table 4.6.

Table 4.6: *Representing three different isotherm model and their parameters*

Isotherm model	**Plot**	**Slope**	**Intercept**	**R^2**
Langmuir	$\frac{C_{inh}}{\theta}$ vs C_{inh}	0.98 ± 0.01	2.76E-04 ± 9.68E-06	0.999
Freundlich	$\ln\theta$ vs $\ln C_{inh}$	0.19 ± 0.02	1.03 ± 0.15	0.971
Temkin	θ vs $\ln C_{inh}$	0.15 ± 0.01	1.83 ± 0.10	0.970

***Note:** For all three isotherm models the surface coverage value (θ) of 3 h immersion was used.

In summary, among the three isotherm models, the adsorption of alkaloids onto the metal surface strictly followed the Langmuir model with the formation of protective monolayers on the equivalent adsorption interfaces through a spontaneous process as suggested by the Freundlich model. The metal then subsequently got protected due to significant adsorption and adhesion ability of the inhibitor compounds to the MS surface forming a protective barrier as suggested by the Temkin model.

4.4 Activation Energy and Corrosion Kinetic

The thermodynamic activation energy was calculated using the collected data from the weight loss method at various temperatures. Which is taken into consideration to study corrosion kinetics. So, from the Arrhenius equation (2.7) activation energy is estimated.

$$\log(\mathrm{CR}) = \log(\mathrm{A}) - \frac{\mathrm{E_a}}{2.303\mathrm{RT}} \tag{2.7}$$

Where,

A = Arrhenius's pre-exponential constant, E_a = Activation energy, and T = Absolute temperature.

A graphical plot of log(CR) on the y-axis and 1/2.303RT on the x-axis was plotted in which a slope of a straight line was obtained. For instance, activation energy was evaluated from that slope. Figure 4.9 is the graphical representation of the Arrhenius plot of this study from which it was found that 48.54 kJ/mol of energy of activation is required for the reaction between MS and the acid solution.

After analyzing the obtained values of slopes, it was found that the activation energy rises from 48.54 kJ/mol to 107.26, 114.14, and 113.14, and reaches 139.28 kJ mol^{-1} in the presence of different concentrations of inhibitor i.e., 200, 400, 600, and 800 ppm respectively. The rise in activation energy suggests a reduction in MS sample dissolution in an acidic media.

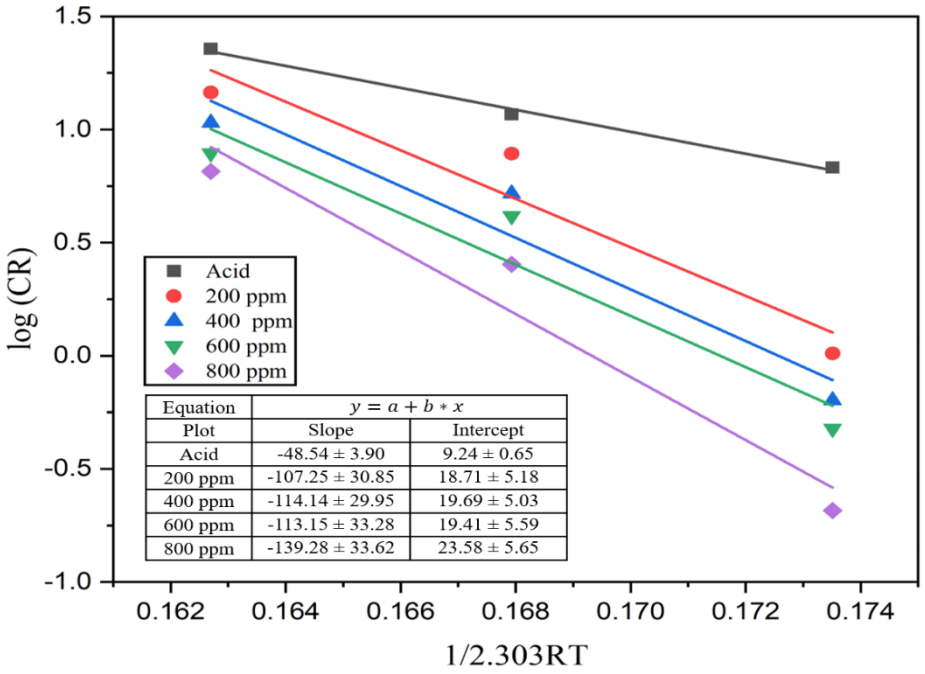

Equation	$y = a + b * x$	
Plot	Slope	Intercept
Acid	-48.54 ± 3.90	9.24 ± 0.65
200 ppm	-107.25 ± 30.85	18.71 ± 5.18
400 ppm	-114.14 ± 29.95	19.69 ± 5.03
600 ppm	-113.15 ± 33.28	19.41 ± 5.59
800 ppm	-139.28 ± 33.62	23.58 ± 5.65

Figure 4.9: *Arrhenius plot for the MS sample in 1M H_2SO_4 and different concentrations of the inhibitor solutions*

4.5 Thermodynamics of Corrosion

The thermodynamics of corrosion is studied from the transition state plots utilizing a transition state equation (2.8). From this equation, the thermodynamic parameters such as enthalpy and entropy of the system were evaluated.

$$\log\left(\frac{\mathrm{CR}}{\mathrm{T}}\right) = \log\left(\frac{\mathrm{R}}{\mathrm{hN}}\right) + \left(\frac{\Delta \mathrm{S}^{\circ}}{2.303\mathrm{R}}\right) - \frac{\Delta \mathrm{H}^{\circ}}{2.303\mathrm{RT}} \qquad (2.8)$$

Where,

h = Plank's constant (6.6261×10^{-34}Js) and N = Avogadro's number (6.0225×10^{23} mol^{-1}). A graphical fitting of $log\left(\frac{CR}{T}\right)$ on the y-axis against $\frac{1}{2.303RT}$ on the x-axis was plotted to obtain a transition state graph. The entropy of activation (ΔS°) is estimated from the intercept of the straight line while the enthalpy of activation (ΔH°) is measured from its slope in acid with and without the presence of inhibitors as presented in Figure 4.10.

.

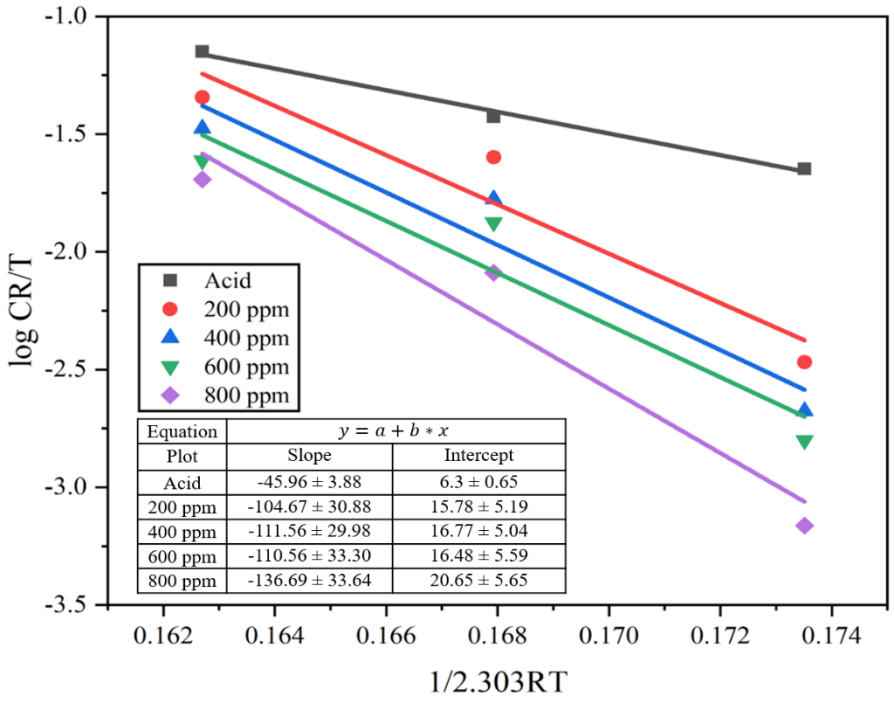

Figure 4.10: *The transition state plot for the MS in acid and different concentrations of the inhibitor solutions*

It was observed that in the presence of an alkaloid, the system's enthalpy (ΔH°) was found to be greater as compared to the enthalpy of the system (ΔH°) in the acid. Also, the enthalpy value steadily rises as the concentration of the inhibitor solution increases between 45.96 to 136.69 kJ mol^{-1}. Here an endothermic adsorption process is indicated by the positive value of Enthalpy's (ΔH°) that subsequently lowers the rate of corrosion (Karki *et al.*, 2021). Additionally, the intercept of the transition state plot is used to determine the entropy of the system (ΔS°). For the different inhibitor concentrations, the entropy value rises from negative 76.63 kJ mol^{-1} of acid solution to the positive entropy values i.e., 104.69, 123.55, 118.08, and 197.96 kJ mol^{-1} respectively as shown in Figure 4.7. As the entropy value changes from negative to positive, this implies a significant value shift. The reason behind this may be due to the formation of activated complexes through an associative mechanism, which in turn increases randomness in the transition state (Ituen *et al.*, 2017; Karki *et al.*, 2022). Moreover, alkaloid molecules substitute the water molecules on the MS surface through a process called quasi-substitution throughout the adsorption process (Oli *et al.*, 2021).

Table 4.7 displayed the calculated values of E_a, ΔS°, and ΔH° from the transition state plot. Here, the E_a value is greater than ΔH°, suggesting a cathodic hydrogen evolution reaction that causes the overall reaction's volume to decrease (Oli *et al.*, 2021). The

mean value of the difference in the activation energy and enthalpy of the system (E_a - $\Delta H°$) is found to be 2.58 kJ mol^{-1}. This closely resembles the value of RT and follows the equation Ea - H° = RT. Alkaloids, therefore, adsorb as a result of physical-dominant chemical adsorption (Ituen *et al.*, 2017; Thapa *et al.*, 2022).

Table 4.7: *Activation parameters of the MS dissolution in 1 M H_2SO_4 without and with inhibitor*

Electrolyte	A (g/cm^2)	E_a (kJ/mol)	ΔH° (kJ/mol)	E_a - ΔH°	ΔS° ($Jmol^{-1}K^{-1}$)
Acid	32.98	48.54	45.96	2.58	-76.63
200 ppm	31.24	107.26	104.67	2.59	104.69
400 ppm	29.21	114.14	111.56	2.58	123.55
600 ppm	30.36	113.14	110.57	2.57	118.08
800 ppm	29.08	139.28	136.70	2.58	197.96

4.6 Electrochemical Measurements

The corrosion kinetics and the nature of the inhibition for the MS specimen in 1 M H_2SO_4 solution in both the presence and absence of different concentrations of alkaloid which is extracted from the stem of AA was further examined by the PDP and EIS measurements at 293 K.

4.6.1 Potentiodynamic polarization tests (PDP)

The previously pretreated MS specimens either with acid or with the different inhibitor solutions of 200, 400, 600, and 800 ppm respectively were placed in an electrochemical setup to record the as-immersed and one-hour immersed polarization curves in the potential window of -0.8 to -0.2 V on the Gamry Framework instrument at 293 K.

a) As-immersed polarization curve

The as-immersed MS sample's anodic and cathodic Tafel polarization curves in acid with and without different concentrations of inhibitor solution are displayed in Figure 4.11. In the graphical plot of as-immersed data, an extrapolation method is used to record the electrochemical characteristics such as corrosion potential, current density, cathodic slope, anodic slope, and inhibition efficiency. This is represented in Table 4.8 which showed a slight variation in the I_{corr} value with increasing concentration. Among the studied inhibitor's concentration range, the MS specimen immersed in 600 and 800 ppm inhibitor showed a comparable equal inhibitory performance.

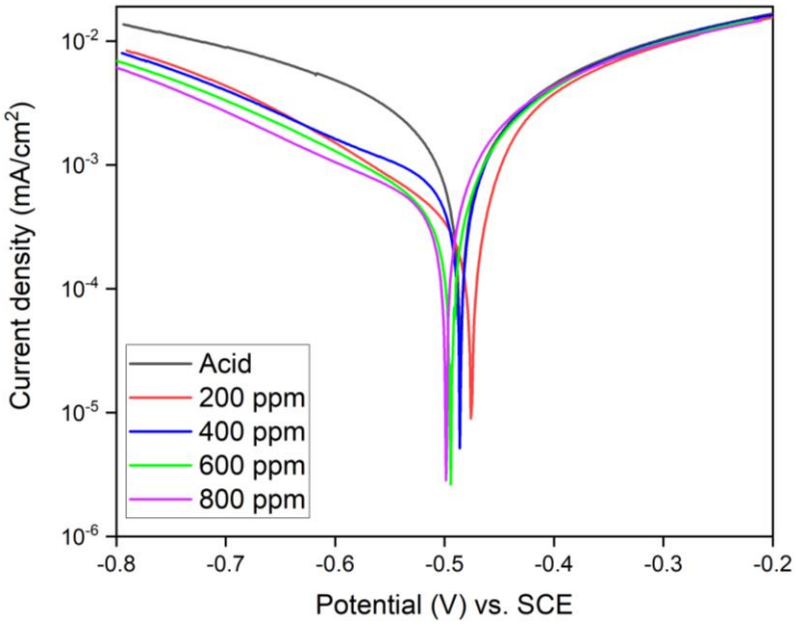

Figure 4.11: *PDP curve for as-immersed MS sample in acid and different concentrations of inhibitor solution at 293 K*

However, the inhibition efficiency is not higher compared to the MS immersed for a one-hour immersion time. This could be due to insufficient time to produce a protective thin film on the interface region between the metal surface and the corrosive environment.

Table 4.8: *Polarizations parameters of as-immersed MS sample in both acid and different concentrations of inhibitor solutions*

Medium	OCP (V)	Current density ($\mu A/cm^2$)	Anodic slope	Cathodic slope	I.E. %
Acid	-0.485	0.984	-9.05 ± 0.13	10.35 ± 0.12	-
200 ppm	-0.475	0.256	-13.69 ±0.22	22.98 ± 0.53	73.98
400 ppm	-0.486	0.268	-12.57 ± 0.15	19.68 ± 011	72.76
600 ppm	-0.494	0.220	-12.48 ± 0.26	21.29 ± 0.24	77.64
800 ppm	-0.499	0.224	-12.13 ± 0.12	23.01 ± 0.21	77.23

b) One hour immersed polarization curve

Similarly, one-hour immersed MS samples' in acid with and without different inhibitor concentrations are displayed in Figure 4.12. After being exposed to acid and inhibitor media, the MS surface exhibited rapid physical adsorption as well as desorption of the inhibitor molecules, which resulted in a decrease in the corrosion current density (I_{corr}) (Karki *et al.*, 2022; Thapa *et al.*, 2022) with the increment in the inhibitor concentrations as seen in Table 4.9.

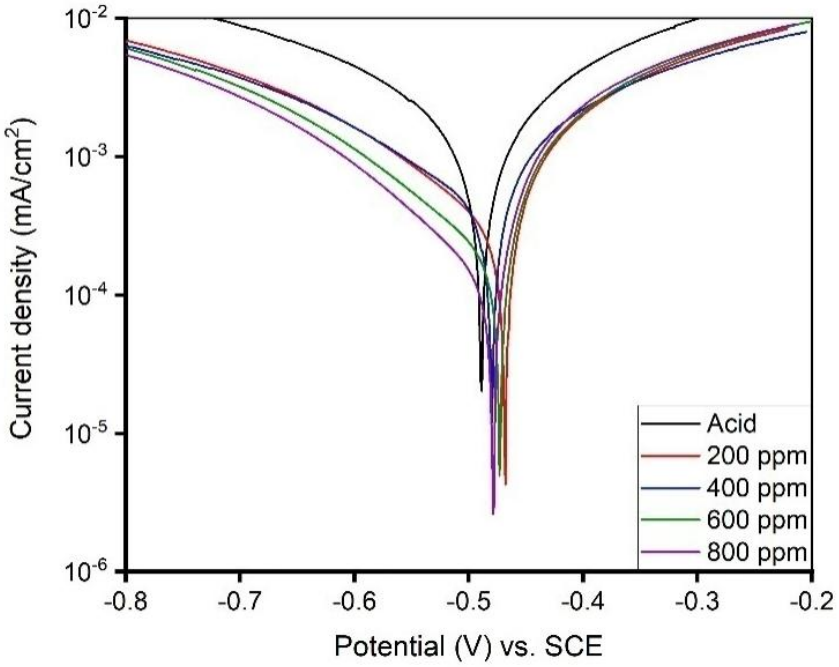

Figure 4.12: *PDP curves for one-hour immersed MS sample in acid and different concentrations of inhibitor solution at 293 K.*

As the inhibitor concentration rose, the Tafel plot of the one-hour immersed MS sample showed a declining I_{corr} value with a corrosion potential between -0.468 to -0.490 V. The 800 ppm inhibitor solution with the lowest current density (I_{corr}) value of 0.10 μA/cm^2 revealed the highest inhibitory performance of 91.23%. Also, there is a declining trend of current density (I_{corr}) values in Table 4.9 with the increasing inhibitor concentrations. This might be a result of the physical adsorption of alkaloids onto the substrate, which lowers the electron transport from the surface and, in turn, lowers the possibility of attack by corrosive ions by increasing resistance (Thapa *et al.*, 2022).

Table 4.9: *Polarization parameters of 1 h immersed MS sample in both acid and different concentrations of inhibitor solutions*

Medium	OCP (V)	Current density (μA/cm^2)	Anodic slope	Cathodic slope	I.E. %
Acid	-0.485	1.14	-5.77 ± 0.05	7.32 ± 0.09	-
200 ppm	-0.468	0.31	-6.14 ± 0.03	12.19 ± 0.24	72.81
400 ppm	-0.480	0.28	-5.83 ± 0.03	18.11 ± 0.41	75.44
600 ppm	-0.472	0.18	-6.67 ± 0.02	13.56 ± 0.37	84.21
800 ppm	-0.478	0.10	-7.31 ± 0.04	20.17 ± 0.60	91.23

4.6.2 Electrochemical Impedance Spectroscopy (EIS)

The EIS measurements were carried out before PDP measurements to estimate the resistance or impedance of the MS sample at both as-immersed and one-hour

immersion conditions. Figures 4.13 (a-c) and 4.14 (a-c) displayed the Nyquist and Bode plots from the EIS investigation, while Figures 4.13 (d) and 4.14 (d) illustrated the corresponding circuit models. In the equivalent circuit model, CPE is a constant phase element which indicates the double-layer capacitance of the metal/solution interface, while Rs stands for solution resistance, and Rct for charge transfer resistance at the metal/solution interface. The actual corrosion system is comprised largely of non-homogenous electrode surfaces. The non-homogeneity is mostly due to the adsorption of inhibitor, the development of a porous layer, and the presence of rough structures on the electrode surface. However, in the model circuit, the CPE makes up for this non-homogeneity (Elmsellem *et al.*, 2014). The impedance function is represented by the equation (Tan *et al.*, 2021);

$$Z_{CPE} = \frac{1}{Q(j\omega)^n} \tag{2.9}$$

Where,

Q = magnitude of the CPE, j = imaginary number, ω = angular frequency, and n = CPE exponent which ranges from -1 to +1 may indicate non-homogeneity (Karki *et al.*, 2021; Tan *et al.*, 2021).

a) As-immersed EIS Plot

The potentiostatic EIS measurement in the as-immersed condition reflected the very initial inhibition capacity of the inhibitor molecules as it was carried out just after recording 99-second open circuit potential. Figure 4.13 (a-c) displayed a gradually increasing single capacitive loop in the Nyquist plot with the rise in the inhibitor's concentration. This indicates that the charge transfer method regulates MS corrosion in an acid solution without altering the mechanism (Alagta *et al.*, 2008). Also, the continuous rise in the diameter of the capacitive loop in the Nyquist plot with increasing inhibitor concentration corresponds to a rise in charge transfer resistance value. This may be due to the surface coverage by the alkaloid molecules (Bentiss *et al.*, 2000).

The calculated impedance values from the Nyquist plot are shown in Table 4.10. The MS sample has an Rct value of 6.99 cm^{-2} in an acidic solution for as-immersion. For the MS sample, the maximum inhibitory performance of 66.05% was seen in an 800 ppm solution, while the least inhibitory performance was seen in a 200 ppm inhibitor

solution. This lowest value of EIS in as-immersed conditions may be due to the very short time for the inhibitor molecules to get adsorbed on the MS surface.

Table 4.10: *EIS parameters for as-immersed analysis derived from the equivalent circuit using Z-view software*

Medium	Rs (Ωcm^2)	CPE ($\mu\Omega S^n cm^{-2}$)	n	Rct(inh) (Ωcm^2)	I.E. %
200 ppm	15.31	83.04	0.892	13.51	49.63
400 ppm	16.80	97.24	0.919	14.23	52.66
600 ppm	16.00	98.22	0.921	16.14	58.20
800 ppm	17.49	130.37	0.881	20.46	66.05

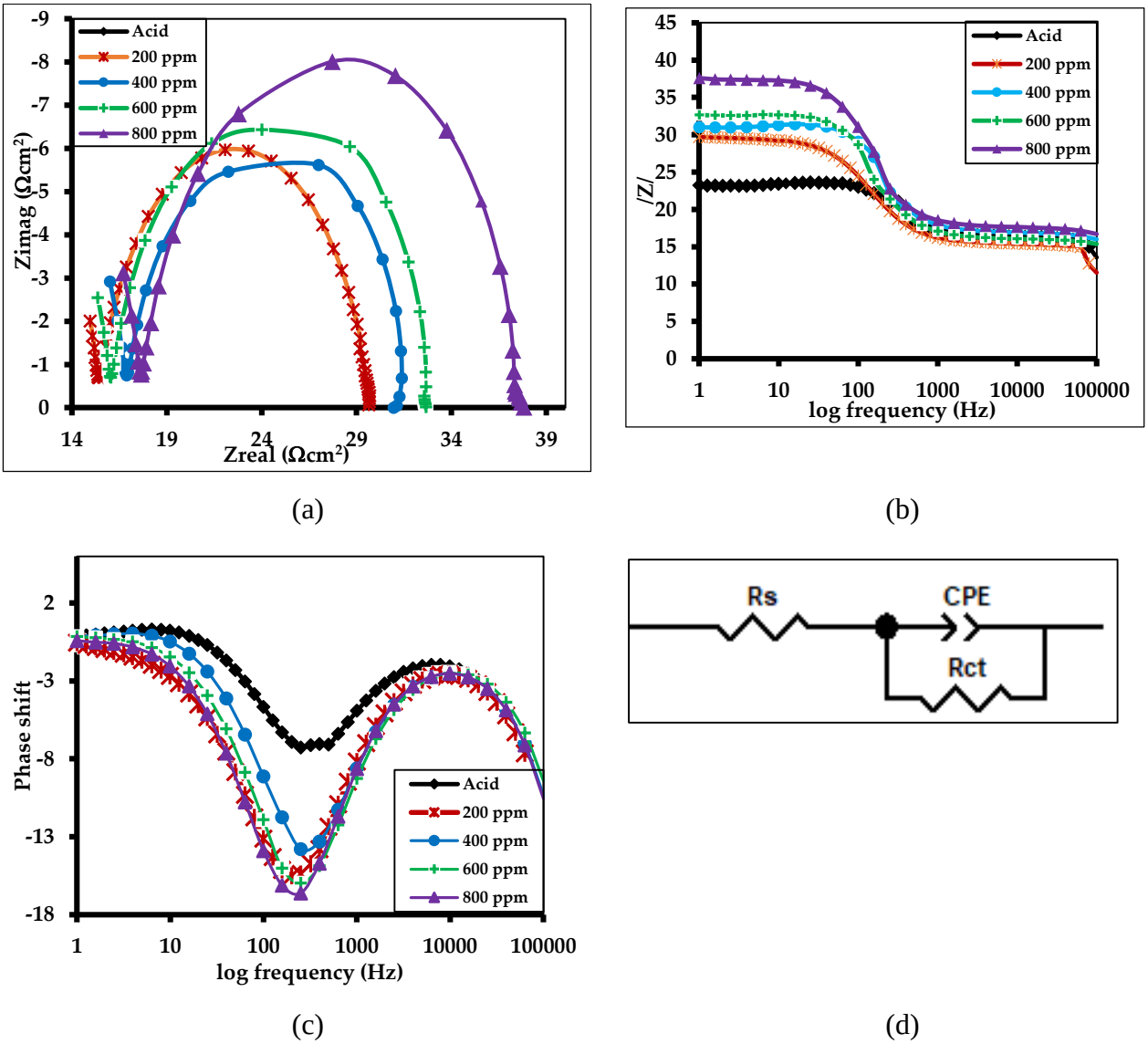

Figure 4.13: *EIS plots; a) Nyquist plot, (b) Phase angle plot in Bode plots, (c) Magnitude plot in Bode plots of phase shift versus log frequency for the as-immersed MS in 1M H_2SO_4 with and without different inhibitor's concentrations, and (d) the impedance spectra fitted using an equivalent circuit model*

b) One-hour immersed EIS plot

The observation revealed a correlation between rising inhibitor molecule concentrations and increasing impedance values as shown in Table 4.11. The MS sample has an Rct value of 6.59 cm^{-2} in an acidic solution for one-hour immersion. The MS sample displayed the highest inhibitory performance of 92.53% in an 800 ppm inhibitor solution, whereas the corresponding MS sample exhibited the lowest inhibitory performance of 58.05% in a 200 ppm inhibitor solution after one-hour immersion. This is because a thin protective layer has formed on the MS surface that blocks or completely eliminates the possibility of corrosive ions or molecules penetrating the surface by raising the interfacial impedance/resistance of the MS sample.

Table 4.11: *EIS parameters for one-hour immersion analysis derived from the equivalent circuit using Z-view software*

Medium	Rs (Ωcm^2)	CPE ($\mu\Omega S^n cm^{-2}$)	n	Rct(inh) (Ωcm^2)	I.E. %
200 ppm	17.31	338.04	0.888	15.71	58.05
400 ppm	17.42	197.07	0.892	21.70	69.63
600 ppm	16.92	184.79	0.858	31.45	79.05
800 ppm	17.51	102.40	0.885	88.25	92.53

From the observation, one capacitive loop in the Nyquist plot (Figure 4.14a) and only a one-time constant in the Bode plot reveals that the charge transfer process regulates the corrosion of MS in 1M H_2SO_4 solution without disrupting the mechanism (Alagta *et al.,* 2008). According to Bentiss *et al.* in the Nyquist plot, the diameters of the capacitive loop rise with the increasing inhibitor's concentrations. As a result, the charge transfer resistance value of the MS surface in inhibitor solution increases as compared to the corresponding MS surface in acid solution indicating the protected and resistive surface to prevent the charge flow (Bentiss *et al.*, 2000). The Bode-phase plot's increased phase angle further supports alkaloids' inhibitive behavior (Hanini *et al.*, 2021; Hegazy *et al.*, 2014).

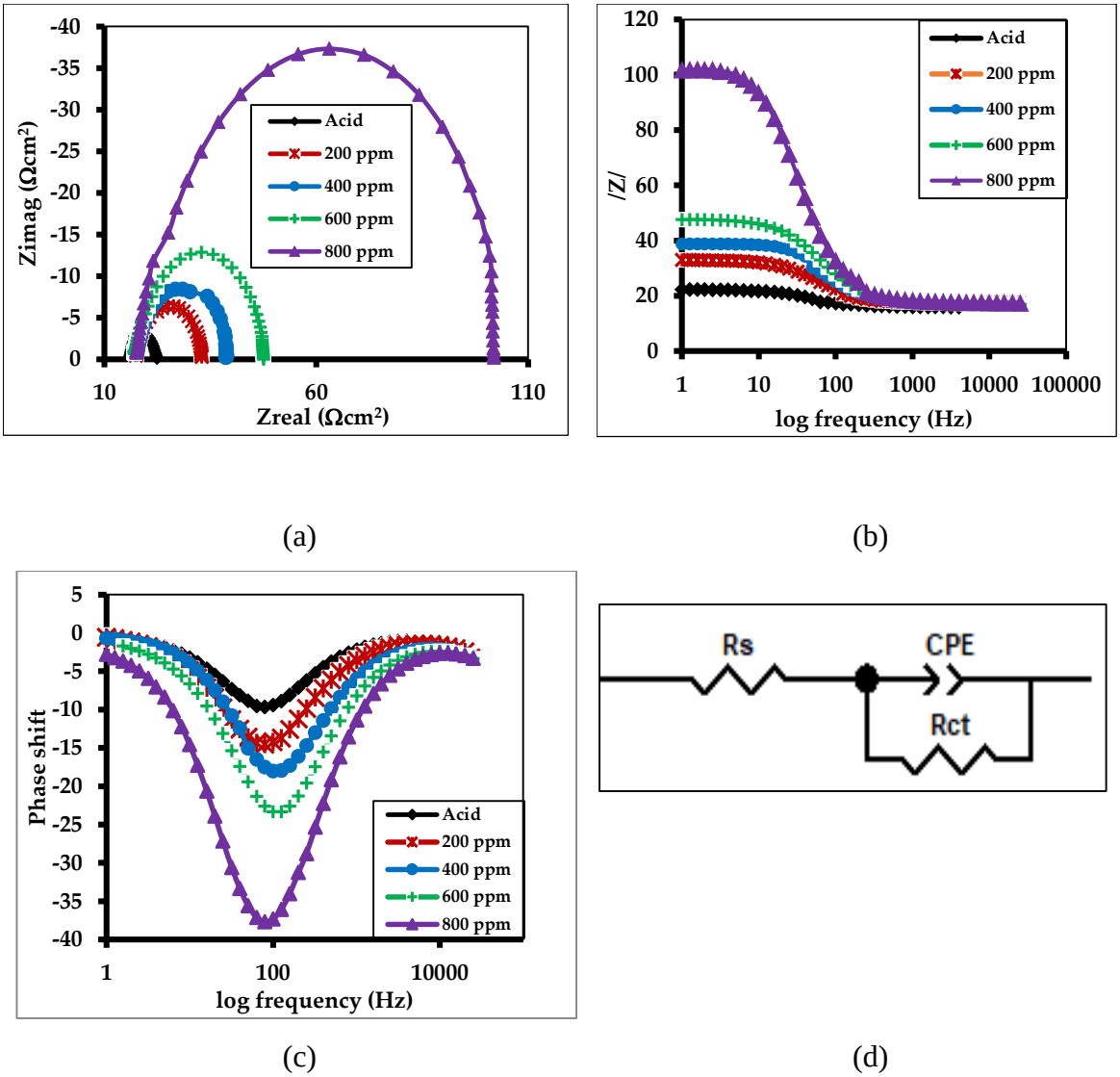

Figure 4.14: *EIS plots; a) Nyquist plot, (b) Phase angle plot in Bode plots, (c) Magnitude plot in Bode plots of phase shift versus log frequency for one-hour immersed MS in 1M H_2SO_4 with and without different inhibitor's concentrations, and (d) the impedance spectra fitted using an equivalent circuit model*

4.7 Discussion and Inhibition Mechanism

The corrosion inhibition mechanism of green inhibitors for MS corrosion can be discussed based on the obtained results. Which is entirely attributed to the adsorptive nature of organic compounds on the MS surface. Mostly, the organic moieties containing polar functional groups along with the hetero-elements are the major reason behind this adsorption phenomenon (Karki *et al.*, 2020; Thapa *et al.*, 2022). In the beginning, the adsorbed negatively charged ions from the MS interface interact with the protonated alkaloid molecules. After that, these molecules release a proton, which causes alkaloid molecules to bind to the MS surface and build thin, protective layers on it (Erami *et al.*, 2019). This corrosion inhibition mechanism is supported by the finding

of electrochemical analysis and thermodynamic values (Oli *et al.*, 2022; Qiang *et al.*, 2018).

From the corrosion kinetics study, the value of activation energy is found to be increasing from 48.54 kJ/mol (for MS in acid) to 139.28 kJ/mol (for MS in 800 ppm inhibitor solution) with the addition of inhibitor. This indicates the increased energy barrier with the decrease in the dissolution of MS in acid media through the alteration in the reaction pathway. Moreover, the Gibbs free energy of adsorption showed that the formation of a thin protective layer is favored and manifested through physicochemical adsorption. Here, the cathodic slope of the polarization curve of the as-immersed sample is quite comparable with the slightest difference in the cathodic slope of one-hour immersion. Therefore, it can be said that the adsorption of the inhibitor molecules onto the MS surface creates a shield or layer that increases the activation energy and prevents the corroding reaction from either at anodic or cathodic sites.

The inhibitory mechanism of alkaloid molecules occurs through the quasi-substitution route. So, simultaneous replacement events occur between the water molecules and inhibitor molecules (Oli *et al.*, 2022).

$$Alk(sol) + xH_2O(ads) === Alk(ads) + H_2O(sol)$$

Here, Alk(sol) and Alk(ads) are used to denote the solvated and adsorbed alkaloid molecules, respectively. While $H_2O(ads)$ is the adsorbed water molecules on the metal surface, and x gives the size ratio representing the number of water molecules replaced by one alkaloid molecule.

The inhibitor molecules are electron-rich organic moieties with a heteroatomic center particularly nitrogen for alkaloids. Such nitrogen centers tend to have high electron density and share their lone pair of electrons from HOMO to the vacant d-orbital of the iron to produce a coordinate covalent bond. This leads to the negative charge accumulation on the metal surface. Then the excess negative charge gets neutralized through the transfer of electrons to the LUMO with the high orbital density thus forming a feedback bond. Such retrodonation phenomenon not only strengthens the bond but also helps in the adsorption of alkaloids.

In this study, the highest estimated corrosion inhibition efficiency in the polarization test is lower than that estimated in the EIS testing, which in turn is lower than the efficiency achieved by the weight loss measurement method. However, such a

difference in the numerical value of inhibition efficiency in all three techniques may be due to systematic and handling errors (Chapagain *et al.*, 2022). Since the EIS measurements are considered the most sensitive and accurate electrochemical technique than the PDP (Komary *et al.*, 2023), the obtained efficiency of inhibitors from this method is acceptable. Inkspace and ChemDraw software were used to sketch the detailed inhibition mechanism which is illustrated in Figure 4.15 below.

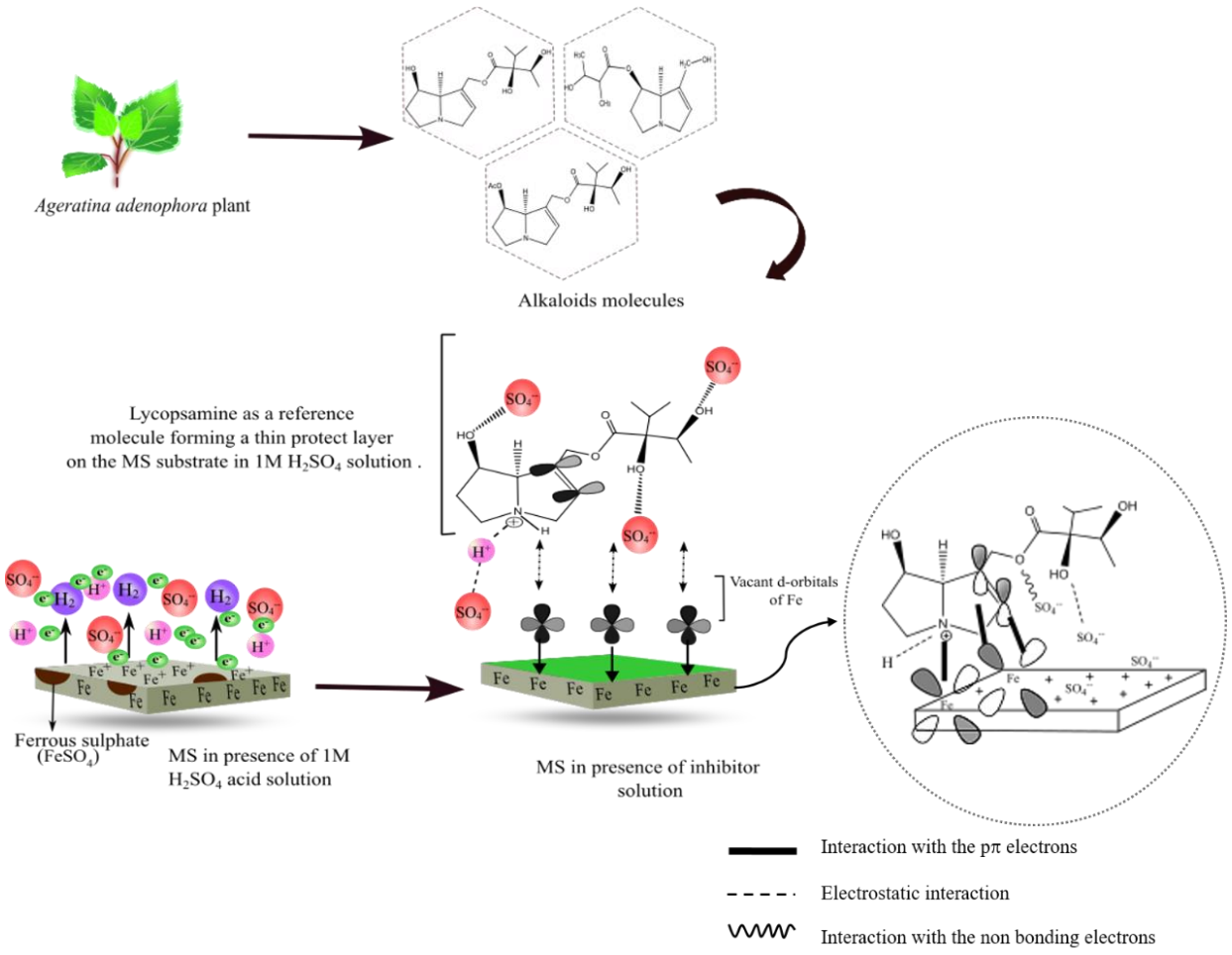

Figure 4.15: *A schematic diagram illustrating the mechanism of alkaloid molecules inhibiting corrosion on MS in 1M H_2SO_4 solution by taking lycopsamine molecule as reference*

CHAPTER 5

CONCLUSION

In this study, alkaloids were successfully separated from *Ageratina adenophora*'s stem to investigate its inhibition efficacy for mild steel corrosion in 1 M H_2SO_4 solution. The extracted alkaloids were characterized by phytochemical screening tests and spectroscopic (UV-Vis and FTIR) methods. For the thorough comparative study of the inhibitory action of alkaloid or inhibitor, the study was carried out by immersing mild steel as a substrate in both acid and different concentrations (200, 400, 600, and 800 ppm) of inhibitors. Various thermodynamic and kinetic parameters were evaluated from the weight loss, EIS, and PDP measurements. From the data analysis, results, and discussions, the findings of this study can be summarized in the following points:

1. The cold percolation method and solvent extraction technique were employed for the extraction of alkaloids from the stem of the AA plant.
2. The characterization of alkaloid molecules in the UV-Vis spectra and FTIR spectra confirmed the presence of various functional groups.
3. From the weight loss and electrochemical measurements, the inhibitory performance of the inhibitor molecule is directly affected by the varying concentrations, immersion time, and operating temperature with the variation in the current density and corrosion potential.
4. The 800 ppm inhibitor solution showed the highest corrosion inhibition efficiency (%) of 96.95% in the EIS measurement at 293K.
5. The inhibitor molecule's adsorptive behavior on the MS interface largely obeys the Langmuir adsorption isotherm model based on the estimated values of K_{ads} and ΔG_{ads}.
6. Moreover, there is a strong interaction between the inhibitor molecules causing spontaneous adsorption as proposed by the Freundlich and Temkin models.

Therefore, it may be concluded that the alkaloid obtained from the *Ageratina adenophora* plant is the potential green inhibitor for mild steel corrosion in one molar sulfuric acid solution.

REFERENCES

Alagta, A., Felhösi, I., Bertoti, I., & Kálmán, E. (2008). Corrosion protection properties of hydroxamic acid self-assembled monolayer on carbon steel. *Corrosion Science*, *50*(6), 1644–1649.

Atrens, A., Chen, X., & Shi, Z. (2022). Mg Corrosion—Recent Progress. *Corrosion and Materials Degradation*, *3*(4), 566–597. https://doi.org/10.3390/cmd3040031

Babbar, N. (2015). An introduction to alkaloids and their applications in pharmaceutical chemistry. *The Pharma Innovation Journal*, *4*(10), 74–75.

Becerra, J., J. (2013). *Phytochemical and analytical studies of feed and medicinal plants in relation to the presence of toxic pyrrolizidine alkaloids* (Doctoral dissertation, Universitäts-und Landesbibliothek Bonn).

Bentiss, F., Traisnel, M., & Lagrenee, M. (2000). The substituted 1, 3, 4-oxadiazoles: a new class of corrosion inhibitors of mild steel in acidic media. *Corrosion Science*, *42*(1), 127–146.

Bhattarai, J. (2010). *Frontiers of Corrosion Science* (1st ed.). Kshitiz Publication.

Breston, J. N. (1952). Corrosion Control with Organic Inhibitors. *Industrial & Engineering Chemistry*, *44*(8), 1755–1761. https://doi.org/10.1021/ie50512a021

Chapagain, A., Acharya, D., Das, A. K., Chhetri, K., Oli, H. B., & Yadav, A. P. (2022). Alkaloid of Rhynchostylis retusa as Green Inhibitor for Mild Steel Corrosion in 1 M H_2SO_4 Solution. *Electrochem*, *3*(2), 211–224. https://doi.org/10.3390/electrochem3020013

Devkota, A., & Das, R. K. (2022). Phytochemical screening and in-vitro evaluation of antimicrobial activity of invasive species Ageratina adenophora collected from Kathmandu valley, Nepal. *Scientific World*, *15*(15), 120–126. https://doi.org/10.3126/sw.v15i15.45660

Elmsellem, H., Nacer, H., Halaimia, F., Aouniti, A., Lakehal, I., Chetouani, A., Al-Deyab, S., Warad, I., Touzani, R., & Hammouti, B. (2014). Anti-corrosive properties and quantum chemical study of (E)-4-methoxy-N-(methoxybenzylidene) aniline and (E)-N-(4-methoxybenzylidene)-4-nitroaniline coating on mild steel in molar hydrochloric. *Int. J. Electrochem. Sci*, *9*(9), 5328–5351.

Erami, R. S., Amirnasr, M., Meghdadi, S., Talebian, M., Farrokhpour, H., & Raeissi, K. (2019). Carboxamide derivatives as new corrosion inhibitors for mild steel protection in hydrochloric acid solution. *Corrosion Science*, *151*, 190–197.

Faiz, M., Zahari, A., Awang, K., & Hussin, H. (2020). Corrosion inhibition on mild steel in 1 M HCl solution by *Cryptocarya nigra* extracts and three of its constituents (alkaloids). *RSC Advances*, *10*(11), 6547–6562. https://doi.org/10.1039/C9RA05654H

Fdil, R., Tourabi, M., Derhali, S., Mouzdahir, A., Sraidi, K., Jama, C., Zarrouk, A., & Bentiss, F. (2018). Evaluation of alkaloids extract of Retama monosperma (L.) Boiss. Stems as a green corrosion inhibitor for carbon steel in pickling acidic medium by means of gravimetric, AC impedance and surface studies. *Journal of Materials and Environmental Sciences*, *9*(1), 358–369. https://doi.org/10.26872/jmes.2018.9.1.39

Fontana, M. G. (1986). *Corrosion engineering* (3rd ed). McGraw-Hill.

Giri, S., Sahu, R., Paul, P., Nandi, G., & Dua, T. K. (2022). An updated review on Eupatorium adenophorum Spreng. [Ageratina adenophora (Spreng.)]: Traditional uses, phytochemistry, pharmacological activities and toxicity. *Pharmacological Research - Modern Chinese Medicine*, *2*, 100068. https://doi.org/10.1016/j.prmcm.2022.100068

Groysman, A. (2010). *Corrosion for everybody*. Springer.

Hanini, K., Benahmed, M., Boudiba, S., Selatnia, I., Akkal, S., & Laouer, H. (2021). Experimental and Theoretical Studies of Taxus Baccata Alkaloid Extract as Eco-Friendly Anticorrosion for Carbon Steel in Acidic Solution. *Protection of Metals and Physical Chemistry of Surfaces*, *57*(1), 222–233. https://doi.org/10.1134/S2070205120060118

Hegazy, M., Abdallah, M., Awad, M., & Rezk, M. (2014). Three novel di-quaternary ammonium salts as corrosion inhibitors for API X65 steel pipeline in acidic solution. Part I: experimental results. *Corrosion Science*, *81*, 54–64.

Hou, B., Li, X., Ma, X., Du, C., Zhang, D., Zheng, M., Xu, W., Lu, D., & Ma, F. (2017). The cost of corrosion in China. *Npj Materials Degradation*, *1*(1), 4. https://doi.org/10.1038/s41529-017-0005-2

Hryniewicz, T., Rokosz, K., & Rokicki, R. (2008). Electrochemical and XPS studies of AISI 316L stainless steel after electropolishing in a magnetic field. *Corrosion Science*, *50*(9), 2676–2681. https://doi.org/10.1016/j.corsci.2008.06.048

Huang, J., Li, Z., Liaw, B. Y., & Zhang, J. (2016). Graphical analysis of electrochemical impedance spectroscopy data in Bode and Nyquist representations. *Journal of Power Sources*, *309*, 82–98. https://doi.org/10.1016/j.jpowsour.2016.01.073

Idouhli, R., Oukhrib, A., Khadiri, M., Zakir, O., Aityoub, A., Abouelfida, A., Benharref, A., & Benyaich, A. (2021). Understanding the corrosion inhibition effectiveness using Senecio anteuphorbium L. fraction for steel in acidic media. *Journal of Molecular Structure*, *1228*, 129478. https://doi.org/10.1016/j.molstruc.2020.129478

Ituen, E., Akaranta, O., & James, A. (2017). *Evaluation of Performance of Corrosion Inhibitors Using Adsorption Isotherm Models: An Overview*. *18*(1), 1–34. https://doi.org/10.9734/CSIJ/2017/28976

Javaherdashti, R. (2000). How corrosion affects industry and life. *Anti-Corrosion Methods and Materials*, *47*(1), 30–34. https://doi.org/10.1108/00035590010310003

Karki, N. (2021). *Development of Green Corrosion Inhibitor for Mild Steel Corrosion in acidic medium A PhD thesis submitted to Central Department of Chemistry*,. Tribhuvan University, Kathmandu, Nepal.

Karki, N., Choudhary, Y., & Yadav, A. P. (2018). Thermodynamic, Adsorption and Corrosion Inhibition Studies of Mild Steel by Artemisia vulgaris Extract from Methanol as Green Corrosion Inhibitor in Acid Medium. *Journal of Nepal Chemical Society*, *39*, 76–85. https://doi.org/10.3126/jncs.v39i0.27041

Karki, N., Neupane, S., Chaudhary, Y., Gupta, D. K., & Yadav, A. P. (2020). Berberis aristata: A highly efficient and thermally stable green corrosion inhibitor for mild steel in acidic medium. *Analytical and Bioanalytical Electrochemistry*, *12*(7), 970–988.

Karki, N., Neupane, S., Gupta, D. K., Das, A. K., Singh, S., Koju, G. M., Chaudhary, Y., & Yadav, A. P. (2021). Berberine isolated from Mahonia nepalensis as an eco-friendly and thermally stable corrosion inhibitor for mild steel in acid medium. *Arabian Journal of Chemistry*, *14*(12), 103423.

Karki, R., Bajgai, A. K., Khadka, N., Thapa, O., Mukhiya, T., Oli, H. B., & Bhattarai, D. P. (2022). Acacia catechu Bark Alkaloids as Novel Green Inhibitors for Mild Steel Corrosion in a One Molar Sulphuric Acid Solution. *Electrochem*, *3*(4), 668–687. https://doi.org/10.3390/electrochem3040044

King, M. J., Davenport, W. G., & Moats, M. S. (2013). *Sulfuric acid manufacture: Analysis, control, and optimization* (2. ed). Elsevier.

Koch, G. (2017). Cost of corrosion. *Trends in Oil and Gas Corrosion Research and Technologies*. Elsevier. 2017, 3-30. https://doi.org/10.1016/B978-0-08-101105-8.00001-2

Komary, M., Komarizadehasl, S., Tošić, N., Segura Pérez, I., Lozano-Galant, J. A., & Turmo, J. (2023). Low-Cost Technologies Used in Corrosion Monitoring. *Sensors*, *23*(3), 1309.

Landolt, D. (2007). *Corrosion and surface chemistry of metals*. CRC Press.

Magar, H. S., Hassan, R. Y. A., & Mulchandani, A. (2021). Electrochemical Impedance Spectroscopy (EIS): Principles, Construction, and Biosensing Applications. *Sensors*, *21*(19), 6578. https://doi.org/10.3390/s21196578

Ngouné, B., Pengou, M., Nouteza, A. M., Nanseu-Njiki, C. P., & Ngameni, E. (2019). Performances of Alkaloid Extract from *Rauvolfia macrophylla* Stapf toward Corrosion Inhibition of C38 Steel in Acidic Media. *ACS Omega*, *4*(5), 9081–9091. https://doi.org/10.1021/acsomega.9b01076

Oli, H. B., Parajuli, D. L., Sharma, S., Chapagain, A., & Yadav, A. P. (2021). Adsorption Isotherm and Activation Energy of Inhibition of Alkaloids on Mild Steel Surface in Acidic Medium. *Amrit Research Journal*, *2*(01), 59–67. https://doi.org/10.3126/arj.v2i01.40738

Oli, H. B., Thapa Magar, J., Khadka, N., Subedee, A., Bhattarai, D. P., & Pant, B. (2022). Coriaria nepalensis Stem Alkaloid as a Green Inhibitor for Mild Steel Corrosion in 1 M H2SO4 Solution. *Electrochem*, *3*(4), 713–727. https://doi.org/10.3390/electrochem3040047

Palaniappan, N., Cole, I., Caballero-Briones, F., Manickam, S., Justin Thomas, K. R., & Santos, D. (2020). Experimental and DFT studies on the ultrasonic energy-assisted extraction of the phytochemicals of *Catharanthus roseus* as green corrosion inhibitors for mild steel in NaCl medium. *RSC Advances*, *10*(9), 5399–5411. https://doi.org/10.1039/C9RA08971C

Pedeferri, P. & Ormellese, M. (2018). *Corrosion Science and Engineering* (p.720). Cham, Switzerland: Springer. https://doi.org/10.1007/978-3-319-97625-9

Petrovic, Z. C. (2016). Catastrophes caused by corrosion. *Vojnotehnicki Glasnik*, *64*(4), 1048–1064. https://doi.org/10.5937/vojtehg64-10388

Rosuman, P. F., & Lirio, L. G. (2016). Alkaloids as Taxonomic Marker of Four Selected Species of Eupatorium Weeds. *SPU Research Journal on Global Education, 1*.

Poudel, A. S., Jha, P. K., Shrestha, B. B., & Muniappan, R. (2019). Biology and management of the invasive weed *Ageratina adenophora* (Asteraceae): Current state of knowledge and future research needs. *Weed Research*, *59*(2), 79–92. https://doi.org/10.1111/wre.12351

Qiang, Y., Zhang, S., Tan, B., & Chen, S. (2018). Evaluation of Ginkgo leaf extract as an eco-friendly corrosion inhibitor of X70 steel in HCl solution. *Corrosion Science*, *133*, 6–16.

Revie, R. W., & Uhlig, H. H. (2008). *Corrosion and corrosion control: An introduction to corrosion science and engineering* (4th ed). Wiley-Interscience.

Roberge, P. R. (2008). *Corrosion engineering: Principles and practice*. McGraw-Hill Education.

Sanyal, B. (1981). Organic compounds as corrosion inhibitors in different environments—A review. *Progress in Organic Coatings*, *9*(2), 165–236. https://doi.org/10.1016/0033-0655(81)80009-X

Sastri, V. S. (2011). *Green corrosion inhibitors: Theory and practice*. John Wiley & Sons.

Setzer, W. N. (2018). The Phytochemistry of Cherokee Aromatic Medicinal Plants. *Medicines*, *5*(4), 121. https://doi.org/10.3390/medicines5040121

Shao, H., Yin, X., Zhang, K., Yang, W., Chen, Y., & Liu, Y. (2022). N-[2-(3-indolyl)ethyl]-cinnamamide synthesized from cinnamomum cassia presl and alkaloid tryptamine as green corrosion inhibitor for Q235 steel in acidic medium. *Journal of Materials Research and Technology*, *20*, 916–933. https://doi.org/10.1016/j.jmrt.2022.07.122

Silverstein, R. M., & Webster, F. X. (2005). *Spectrometric identification of organic compounds* (6th ed). John Wiley & Sons.

Singh, W. P., & Bockris, J. O. (1996). Toxicity issues of organic corrosion inhibitors: Applications of QSAR model. In *CORROSION 96*. OnePetro.

Tan, B., Zhang, S., He, J., Li, W., Qiang, Y., Wang, Q., Xu, C., & Chen, S. (2021). Insight into anti-corrosion mechanism of tetrazole derivatives for X80 steel in 0.5 M H_2SO_4 medium: Combined experimental and theoretical researches.

Journal of Molecular Liquids, *321*, 114464. https://doi.org/10.1016/j.molliq.2020.114464

Thapa, A., Pokharel, A., Karki, H., Yadav, R. K., Paudel, N., Bharati, S., Shrestha, T., Maharjan, B., Karanjit, S., & Shrestha, R. L. (2022). Phytochemical Analysis, Cytotoxicity, Antibacterial and Antioxidant Activities of Extracts of Leaf of Ageratina adenophora (Spreng.). *Amrit Research Journal*, *3*(01), 84–93. https://doi.org/10.3126/arj.v3i01.50500

Thapa, O., Thapa Magar, J., Oli, H. B., Rajaure, A., Nepali, D., Bhattarai, D. P., & Mukhiya, T. (2022). Alkaloids of Solanum xanthocarpum Stem as Green Inhibitor for Mild Steel Corrosion in One Molar Sulphuric Acid Solution. *Electrochem*, *3*(4), 820–842. https://doi.org/10.3390/electrochem3040054

Toor, M., & Jin, B. (2012). Adsorption characteristics, isotherm, kinetics, and diffusion of modified natural bentonite for removing diazo dye. *Chemical Engineering Journal*, *187*, 79–88. https://doi.org/10.1016/j.cej.2012.01.089

Ugi, B. U., Bassey, V. M., Obeten, M. E., Adalikwu, S. A., & Nandi, D. O. (2020). Secondary Plant Metabolites of Natural Product Origin—Strongylodon macrobotrys as Pitting Corrosion Inhibitors of Steel around Heavy Salt Deposits in Gabu, Nigeria. *Journal of Materials Science and Chemical Engineering*, *8*(5), 38–60. https://doi.org/10.4236/msce.2020.85004

Verma, C., Ebenso, E. E., & Quraishi, M. A. (2019). Alkaloids as green and environmental benign corrosion inhibitors: An overview. *International Journal of Corrosion and Scale Inhibition*, *8*(3), 512–528.

Verma, C., Verma, D. K., Ebenso, E. E., & Quraishi, M. A. (2018). Sulfur and phosphorus heteroatom-containing compounds as corrosion inhibitors: An overview. *Heteroatom Chemistry*, *29*(4), e21437. https://doi.org/10.1002/hc.21437

Voevodin, N. N., Balbyshev, V. N., Khobaib, M., & Donley, M. S. (2003). Nanostructured coatings approach for corrosion protection. *Progress in Organic Coatings*, *47*(3–4), 416–423. https://doi.org/10.1016/S0300-9440(03)00131-0

Wan, F., Liu, W., Guo, J., Qiang, S., Li, B., Wang, J., Yang, G., Niu, H., Gui, F., Huang, W., Jiang, Z., & Wang, W. (2010). Invasive mechanism and control strategy of Ageratina adenophora (Sprengel). *Science China Life Sciences*, *53*(11), 1291–1298. https://doi.org/10.1007/s11427-010-4080-7

Wang, J., & Guo, X. (2020). Adsorption isotherm models: Classification, physical meaning, application and solving method. *Chemosphere*, *258*, 127279. https://doi.org/10.1016/j.chemosphere.2020.127279

Yu, G., Ma, C., & Li, J. (2020). Flame retardant effect of cytosine pyrophosphate and pentaerythritol on polypropylene. *Composites Part B: Engineering*, *180*, 107520. https://doi.org/10.1016/j.compositesb.2019.107520

Zhao, M., Lu, X., Zhao, H., Yang, Y., Hale, L., Gao, Q., Liu, W., Guo, J., Li, Q., Zhou, J., & Wan, F. (2019). Ageratina adenophora invasions are associated with microbially mediated differences in biogeochemical cycles. *Science of The Total Environment*, *677*, 47–56. https://doi.org/10.1016/j.scitotenv.2019.04.330

Zhou, Z. Y., Liu, W. X., Pei, G., Ren, H., Wang, J., Xu, Q. L., Xie, H. H., Wan, F. H., & Tan, J. W. (2013). Phenolics from *Ageratina adenophora* Roots and Their Phytotoxic Effects on *Arabidopsis thaliana* Seed Germination and Seedling Growth. *Journal of Agricultural and Food Chemistry*, *61*(48), 11792–11799. https://doi.org/10.1021/jf400876j

ALKALOID EXTRACT OF AGERATINA ADENOPHORA STEM ...

By: Jamuna Thapa Magar

As of: Jun 24, 2023 8:03:10 PM
15,976 words - 103 matches - 4 sources

Similarity Index
11%

Mode: Summary Report

sources:

1,142 words / 8% - from 06-Jun-2023 12:00AM
WWW.MDPI.COM

222 words / 2% - Crossref
Jamuna Thapa Magar, Indra Kumari Budhathoki, Anil Rajaure, Hari Bhakta Oli, Deval Prasad Bhattarai, "Alkaloid Extract of Ageratina adenophora Stem as Green Inhibitor for Mild Steel Corrosion in One Molar Sulfuric Acid Solution", Electrochem, 2023

74 words / 1% - from 18-Mar-2023 12:00AM
WWW.MDPI.COM

98 words / 1% - Internet from 25-Aug-2020 12:00AM
mafiadoc.com

paper text:

ALKALOID EXTRACT OF AGERATINA ADENOPHORA STEM AS GREEN CORROSION **INHIBITOR FOR MILD STEEL CORROSION IN** 1M H2SO4 **ACID SOLUTION**

A DISSERTATION WORK **SUBMITTED FOR THE PARTIAL FULFILLMENT OF THE REQUIREMENTS FOR THE** MASTER **OF SCIENCE DEGREE IN CHEMISTRY** SUBMITTED **BY**

: Name: JAMUNA THAPA MAGAR T.U. Examination Roll No.: 1881/076 T.U. Registration No: 5-2-33-238-2014

SUBMITTED TO:

DEPARTMENT OF CHEMISTRY AMRIT CAMPUS **INSTITUTE OF SCIENCE AND TECHNOLOGY KATHMANDU, NEPAL** June 2023 **BOARD OF EXAMINER AND CERTIFICATE OF APPROVAL This dissertation entitled**

."

Alkaloid Extract of Ageratina adenophora Stem as Green Corrosion **Inhibitor for Mild Steel Corrosion in**